

WCAP-11382

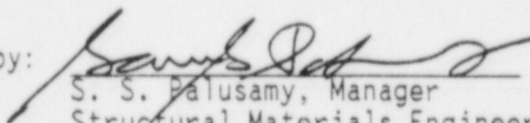
TECHNICAL BASES FOR ELIMINATING CLASS 1
ACCUMULATOR LINE RUPTURE AS
THE STRUCTURAL DESIGN BASIS FOR
SOUTH TEXAS PROJECT UNITS 1 AND 2

January, 1987

S. A. Swamy
F. J. Witt
Y. S. Lee
D. H. Roarty

Verified by: E. R. Johnson

Approved by:


S. S. Palusamy, Manager
Structural Materials Engineering

Work Performed Under Shop Order HPLJ-2028

WESTINGHOUSE ELECTRIC CORPORATION
Generation Technology Systems Division
P.O. Box 2728
Pittsburgh, Pennsylvania 15230-2728

TABLE OF CONTENTS

<u>Section</u>	<u>Title</u>	<u>Page</u>
1.0	INTRODUCTION	1-1
	1.1 Background	1-1
	1.2 Scope and Objective	1-1
	1.3 References	1-4
2.0	FAILURE MECHANISMS FOR FLAWED PIPES	2-1
	2.1 General Considerations	2-1
	2.2 Global Failure Mechanism	2-1
	2.3 Local Failure Mechanism	2-2
	2.4 References	2-3
3.0	OPERATION AND STABILITY OF THE ACCUMULATOR LINES AND THE REACTOR COOLANT SYSTEM	3-1
	3.1 Stress Corrosion Cracking	3-1
	3.2 Water Hammer	3-3
	3.3 Low Cycle and High Cycle Fatigue	3-4
	3.4 References	
4.0	MATERIAL CHARACTERIZATION	4-1
	4.1 Pipe, Fittings and Weld Materials	4-1
	4.2 Tensile Properties	4-2
	4.3 Fracture Toughness Properties	4-3
	4.4 References	4-4
5.0	LOADS FOR FRACTURE MECHANICS ANALYSIS	5-1
	5.1 Loads for Crack Stability Analysis	5-2
	5.2 Loads for Leak Rate Evaluation	5-2
	5.3 Summary of Loads Geometry and Materials	5-3

TABLE OF CONTENTS (cont.)

<u>Section</u>	<u>Title</u>	<u>Page</u>
6.0	FRACTURE MECHANICS EVALUATION	6-1
	6.1 Global Failure Mechanism	6-1
	6.2 Leak Rate Predictions	6-3
	6.3 Local Failure Mechanism	6-5
	6.4 References	6-7
7.0	ASSESSMENT OF FATIGUE CRACK GROWTH	7-1
	7.1 Acceptability of Fatigue Crack Growth	7-2
	7.2 References	7-3
8.0	ASSESSMENT OF MARGINS	8-1
9.0	CONCLUSIONS	9-1
APPENDIX A	Limit Moment	A-1
APPENDIX B	Fatigue Crack Growth Considerations	B-1
B.1	Thermal Transient Stress Analysis	B-2
B.2	Fatigue Crack Growth Analysis	B-7
B.3	References	B-10

LIST OF FIGURES

<u>Figure</u>	<u>Title</u>	<u>Page</u>
2-1	Schematic of Generalized Load Deformation Behavior	2-4
5-1	Schematic Layout of Accumulator Line Loop 1	5-6
5-2	Schematic Layout of Accumulator Line Loop 2	5-7
5-3	Schematic Layout of Accumulator Line Loop 3	5-8
6-1	[σ] ^{a,c,e} Stress Distribution	6-8
6-2	Loads Acting on the Pipe Model	6-9
6-3	"Critical" Flaw Size Prediction	6-10
6-4	Analytical Predictions of Critical Flaw Rates of Steam - Water Mixtures	6-11
6-5	[σ] ^{a,c,e} Pressure Ratio as a Function of L/D	6-12
6-6	Idealized Pressure Drop Profile Through a Postulated Crack	6-13
6-7	Leak Rate Versus Crack Length	6-14
A-1	Pipe with a Through Wall Crack in Bending	A-2
B-1	Comparison of Typical Maximum and Minimum Stress Profile Computed by Simplified [σ] ^{a,c,e}	B-15

LIST OF FIGURES (cont.)

<u>Figure</u>	<u>Title</u>	<u>Page</u>
B-2	Schematic of Accumulator Line at [] ^{a,c,e}	B-16
B-3	[^{a,c,e} Maximum and Minimum Stress Profile for Transient #10	B-17
B-4	[^{a,c,e} Maximum and Minimum Stress Profile for Transient #11	B-18
B-5	[^{a,c,e} Maximum and Minimum Stress Profile for Transient #12	B-19
B-6	[^{a,c,e} Maximum and Minimum Stress Profile for Transient #14	B-20

LIST OF TABLES

<u>Table No.</u>	<u>Title</u>	<u>Page</u>
4-1	Room Temperature Mechanical Properties of the High Pressure Accumulator Line Materials and Welds of the South Texas Project Unit 1 Plant	4-4
4-2	Room Temperature Mechanical Properties of the High Pressure Accumulator Line Materials and Welds of the South Texas Project Unit 2 Plant	4-7
4-3	Room Temperature Tensile Properties of the SA351 CF8A Cast 45 Degree Nozzle	4-10
4-4	Typical Tensile Properties of SA376 TP316, SA351 CF8A and Welds of Such Material for the Primary Loop	4-11
4-5	Comparison of Tensile Properties of the 12-Inch High Energy Accumulator Lines With Those of Typical Wrought Primary Loops	4-12
4-6	Fracture Toughness Properties Typical of the Accumulator Line	4-13
4-7	Chemistry and ends of Service Life KCU Toughness for the Six 45° Nozzles	4-14
5-1	Summary of Envelope Loads	5-4
5-2	Loading Components at Governing Locations	5-5
8-1	Comparison of Results vs. Criteria	8-3

LIST OF TABLES (cont.)

<u>Table No.</u>	<u>Title</u>	<u>Page</u>
B-1	Thermal Transients Considered for Fatigue Crack Growth Evaluation	B-12
B-2	Stresses for the Minor Transients (PSI)	B-13
B-3	Accumulator Line Fatigue Crack Growth Results	B-14

SECTION 1.0

INTRODUCTION

1.1 Background

The current structural design basis for the accumulator line* requires postulating non-mechanistic circumferential and longitudinal pipe breaks. This results in additional plant hardware (e.g. pipe whip restraints and jet shields) which would mitigate the dynamic consequences of the pipe breaks. It is, therefore, highly desirable to be realistic in the postulation of pipe breaks for the accumulator line. Presented in this report are the descriptions of a mechanistic pipe break evaluation method and the analytical results that can be used for establishing that a circumferential type break will not occur within the Class 1 portions of the accumulator lines. The evaluations considering circumferentially oriented flaws cover longitudinal cases, and thereby eliminate the need for some of the plant hardware.

1.2 Scope and Objective

The general purpose of this investigation is to demonstrate leak-before-break for the accumulator line. Schematic drawings of the piping system are shown in Section 5.0. The recommendation and criteria proposed in NUREG 1061 Volume 3 (1-1) are used in this evaluation. These criteria and resulting steps of the evaluation procedure can be briefly summarized as follows:

- 1) Calculate the applied loads. Identify the location at which the highest stress occurs.
- 2) Identify the materials and the associated material properties.

* The scope of this work covers that Class 1 portion of the Emergency Core Cooling System from the RCS cold leg injection points to the first check valve.

- 3) Postulate a surface flaw at the governing location. Determine fatigue crack growth. Show that a through-wall crack will not result.
- 4) Postulate a through-wall flaw at the governing location. The size of the flaw should be large enough so that the leakage is assured of detection with margin using the installed leak detection equipment when the pipe is subjected to normal operating loads. Typical plants are equipped with leak detection systems capable of detecting a leakage of 1 gpm as required by the Regulatory Guide 1.45. If a margin of 10 is retained between the calculated leak rate and the leak detection capability, the postulated flaw is required to yield at least 10 gallons per minute leakage when subjected to normal operating loads.
- 5) Using normal plus SSE loads, demonstrate that there is a margin of at least 2 between the leakage size flaw and the critical size flaw.
- 6) Review the operating history to ascertain that operating experience has indicated no particular susceptibility to failure from the effects of corrosion, water hammer or low and high cycle fatigue.
- 7) For the base and weld metals actually in the plant provide the material properties including toughness and tensile test data. Justify that the properties used in the evaluation are representative of the plant specific material. Evaluate long term effects such as thermal aging where applicable.
- 8) Demonstrate margin on applied load.

The flaw stability criteria proposed for the analysis will examine both the global and local stability for a postulated through-wall circumferential flaw. The global analysis is carried out using the []^{a,c,e} method, based on traditional plastic limit load concepts, but accounting for []^{a,c,e} and taking into account the presence of a flaw. The

Local stability analysis can be carried out using the method described in NUREG/CR 3464 (1-2). This method is based on linear elastic fracture mechanics and it can be used up to load levels producing stresses near the yield point. For higher loads, the local stability analysis is carried out by performing a static elastic-plastic [

] ^{a,c,e} of a straight piece of the accumulator line pipe containing a through-wall circumferential flaw.

The leak rate is calculated for the normal operating condition. The leak rate prediction model used in this evaluation is an [

] ^{a,c,e} The crack opening area required for calculating the leak rates is obtained by subjecting the postulated through-wall flaw to normal operating loads. Surface roughness is accounted for in determining the leak rate through the postulated flaw.

As stated earlier, the evaluations described above considering circumferentially oriented flaws cover longitudinal cases in pipes and elbows. The likelihood of a split in the elbows is very low because of the fact that the elbows are [] ^{a,c,e} and no flaws are actually anticipated. The prediction methods for failure in elbows are virtually the same as those for [

] ^{a,c,e} However, the elbows are [] ^{a,c,e} and, therefore, the probability of any longitudinal flaw existing in the accumulator line is much smaller when compared with the circumferential direction. Based on the above, it is judged that circumferential flaws are more limiting than longitudinal flaws in elbows and throughout the system.

The computer codes used in this evaluation for leak rate and fracture mechanics calculations have been validated (bench marked) as described in References (1-4) and (1-5).

1.3 References

- 1-1 Report of the U.S. Nuclear Regulatory Commission Piping Review Committee - Evaluation of Potential for Pipe Breaks, NUREG 1061, Volume 3, November 1984.
- 1-2 NUREG/CR-3464, 1983, "The Application of Fracture Proof Design Methods Using Tearing Instability Theory to Nuclear Piping Postulated Circumferential Through Wall Cracks."
- 1-3 Begley, J.A., et. al., "Crack Propagation Investigation Related to the Leak-Before-Break Concept for LMFBR Piping" in Proceedings, Conference on Elastic Plastic Fracture, Institution of Mechanical Engineers, London 1978.
- 1-4 Swamy, S.A., et. al., "Additional Information in Support of the Elimination of Postulated Pipe Ruptures in the Pressurizer Surge Lines of South Texas Project Units 1 and 2" WCAP-11256, September 1986, Westinghouse Proprietary Class 2.
- 1-5 Swamy, S. A., et. al., "Technical Basis for Eliminating Pressurizer Surge Line Ruptures as the Structural Design Basis for South Texas Project Units 1 and 2," WCAP-11256 Supplement 1, November 1986, Westinghouse Proprietary Class 2.

SECTION 2.0

FAILURE CRITERIA FOR FLAWED PIPES

2.1 General Considerations

Active research is being carried out in industry and universities as well as other research organizations to establish fracture criteria for ductile materials. Criteria being investigated include those based on J-integral initiation toughness, equivalent energy, crack opening displacement, crack opening stretch, crack opening angle, net-section yield, tearing modulus and void nucleation. Several of these criteria are discussed in an ASTM publication (2-1).

A practical approach based on the ability to obtain material properties and to make calculations using the available tools was used in selecting the criteria for this investigation. The ultimate objective is to show that the accumulator line containing a conservatively assumed circumferential through-wall flaw is stable under the worst combination of postulated faulted and operating condition loads within acceptable engineering accuracy. With this viewpoint, two mechanisms of failure, namely, local and global failure mechanisms are considered.

2.2 Global Failure Mechanism

For a tough ductile material which is notch insensitive the global failure will be governed by plastic collapse. Extensive literature is available on this subject. A PVRC study (2-2), reviews the literature as well as data from several tests on piping components, and discusses the details of analytical methods, assumptions and methods of correlating experiments and analysis.

A schematic description of the plastic behavior and the definition of plastic load is shown in Figure 2-1. For a given geometry and loading, the plastic load is defined to be the peak load reached in a generalized load versus displacement plot and corresponds to the point of instability.

A simplified version of this criterion, namely, net section yield criterion has been successfully used in the prediction of the load carrying capacity of pipes containing gross size through-wall flaws (2-3) and was found to correlate well with experiment. This criterion can be summarized by the following relationship:

$$W_a < W_p \quad (2-1)$$

where W_a = applied generalized load

W_p = calculated generalized plastic load

W_p represents the load carrying capacity of the cracked structure and it can be obtained by an elastic-plastic finite element analysis or by empirical correlation which is based on the material flow properties as discussed in Section 6.1

2.3 Local Failure Mechanism

The local mechanism of failure is primarily dominated by the crack tip behavior in terms of crack-tip blunting, initiation, extension and finally crack instability. The material properties and geometry of the pipe, flaw size, shape and loadings are parameters used in the evaluation of local failure.

The stability will be assumed if the crack does not initiate at all. It has been demonstrated that the initiation toughness, measured in terms of J_{IN} from a J-integral resistance curve, is a material parameter defining the crack initiation. If, for a given load, the calculated J-integral value is shown to be less than J_{IN} of the material, then the crack will not initiate.

If the initiation criterion is not met, one can calculate the tearing modulus as defined by the following relation:

$$T_{app} = \frac{dJ}{da} \frac{E}{\sigma_f^2} \quad (2-2)$$

where T_{app} = applied tearing modulus
 E = modulus of elasticity
 σ_f = flow stress = []^{a,c,e}
 a = crack length
 σ_y, σ_u = yield and ultimate strength of the material
 respectively.

In summary, the local crack stability will be established by the two-step criteria:

$$J < J_{IN}, \text{ or} \quad (2-3)$$

$$T_{app} < T_{mat}, \text{ if } J \geq J_{IN} \quad (2-4)$$

2.4 References

- 2-1 J.D. Landes, et al., Editors, Elastic-Plastic Fracture, STP-668, ASTM, Philadelphia, PA 19109, November 1977.
- 2-2 J. C. Gerdeen, "A Critical Evaluation of Plastic Behavior Data and a Unified Definition of Plastic Loads for Pressure Components," Welding Research Council Bulletin No. 254.
- 2-3 Mechanical Fracture Predictions for Sensitized Stainless Steel Piping with Circumferential Cracks, EPRI-NP-192, September 1976.

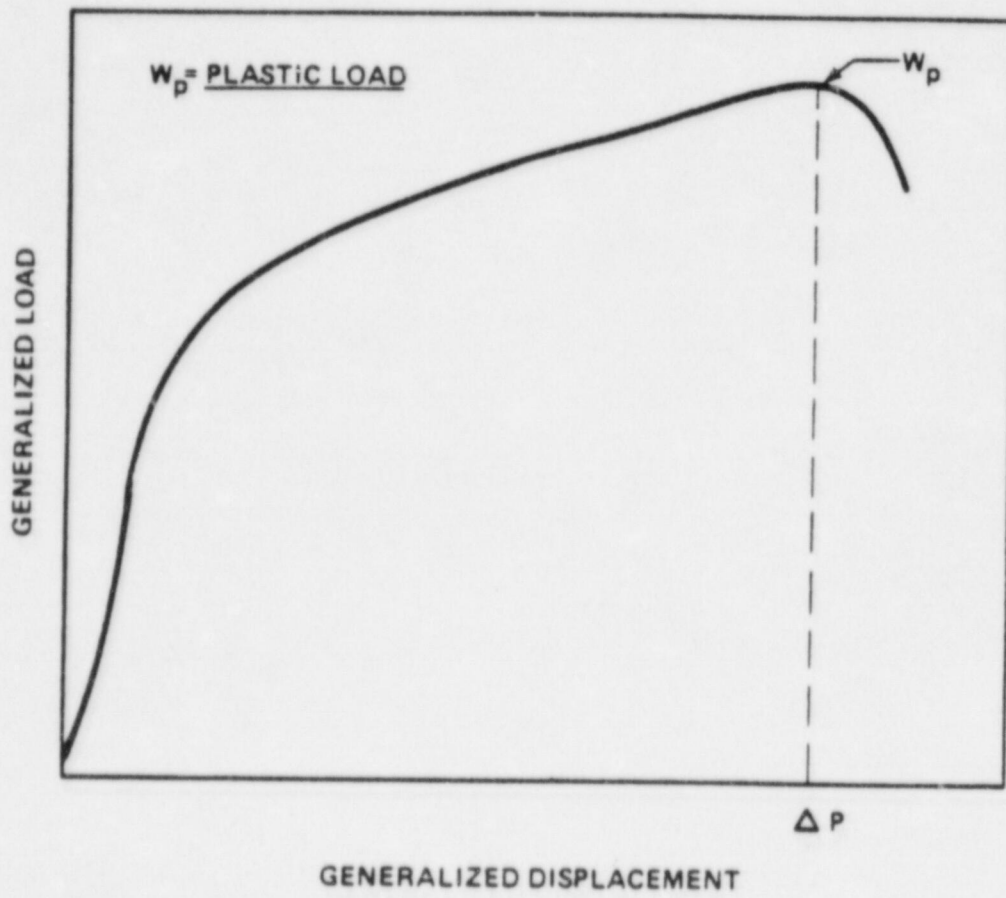


FIGURE 2-1 Schematic of Generalized Load-Deformation Behavior

SECTION 3.0

OPERATION AND STABILITY OF THE ACCUMULATOR LINES AND THE REACTOR COOLANT SYSTEM

3.1 Stress Corrosion Cracking

The Westinghouse reactor coolant system primary loop and connecting Class 1 lines have an operating history that demonstrates the inherent operating stability characteristics of the design. This includes a low susceptibility to cracking failure from the effects of corrosion (e.g., intergranular stress corrosion cracking). This operating history totals over 400 reactor-years, including five plants each having over 15 years of operation and 15 other plants each with over 10 years of operation.

In 1978, the United States Nuclear Regulatory Commission (USNRC) formed the second Pipe Crack Study Group. (The first Pipe Crack Study Group established in 1975 addressed cracking in boiling water reactors only.) One of the objectives of the second Pipe Crack Study Group (PCSG) was to include a review of the potential for stress corrosion cracking in Pressurized Water Reactors (PWR's). The results of the study performed by the PCSG were presented in NUREG-0531 (Reference 3-1) entitled "Investigation and Evaluation of Stress Corrosion Cracking in Piping of Light Water Reactor Plants." In that report the PCSG stated:

"The PCSG has determined that the potential for stress-corrosion cracking in PWR primary system piping is extremely low because the ingredients that produce IGSCC are not all present. The use of hydrazine additives and a hydrogen overpressure limit the oxygen in the coolant to very low levels. Other impurities that might cause stress-corrosion cracking,

such as halides or caustic, are also rigidly controlled. Only for brief periods during reactor shutdown when the coolant is exposed to the air and during the subsequent startup are conditions even marginally capable of producing stress-corrosion cracking in the primary systems of PWRs. Operating experience in PWRs supports this determination. To date, no stress-corrosion cracking has been reported in the primary piping or safe ends of any PWR."

During 1979, several instances of cracking in PWR feedwater piping led to the establishment of the third PCSG. The investigations of the PCSG reported in NUREG-0691 (Reference 3-2) further confirmed that no occurrences of IGSCC have been reported for PWR primary coolant systems.

As stated above, for the Westinghouse plants there is no history of cracking failure in the reactor coolant system loop or connecting Class 1 piping. The discussion below further qualifies the PCSG's findings.

For stress corrosion cracking (SCC) to occur in piping, the following three conditions must exist simultaneously: high tensile stresses, susceptible material, and a corrosive environment. Since some residual stresses and some degree of material susceptibility exist in any stainless steel piping, the potential for stress corrosion is minimized by properly selecting a material immune to SCC as well as preventing the occurrence of a corrosive environment. The material specifications consider compatibility with the system's operating environment (both internal and external) as well as other material in the system, applicable ASME Code rules, fracture toughness, welding, fabrication, and processing.

The elements of a water environment known to increase the susceptibility of austenitic stainless steel to stress corrosion are: oxygen, fluorides, chlorides, hydroxides, hydrogen peroxide, and reduced forms of sulfur (e.g., sulfides, sulfites, and thionates). Strict pipe cleaning standards prior to operation and careful control of water chemistry during plant operation are used to prevent the occurrence of a corrosive environment. Prior to being put

into service, the piping is cleaned internally and externally. During flushes and preoperational testing, water chemistry is controlled in accordance with written specifications. Requirements on chlorides, fluorides, conductivity, and pH are included in the acceptance criteria for the piping.

During plant operation, the reactor coolant water chemistry is monitored and maintained within very specific limits. Contaminant concentrations are kept below the thresholds known to be conducive to stress corrosion cracking with the major water chemistry control standards being included in the plant operating procedures as a condition for plant operation. For example, during normal power operation, oxygen concentration in the RCS and connecting Class 1 lines is expected to be in the ppb range by controlling charging flow chemistry and maintaining hydrogen in the reactor coolant at specified concentrations. Halogen concentrations are also stringently controlled by maintaining concentrations of chlorides and fluorides within the specified limits. This is assured by controlling charging flow chemistry. Thus during plant operation, the likelihood of stress corrosion cracking is minimized.

3.2 Water Hammer

Overall, there is a low potential for water hammer in the RCS and connecting accumulator lines since they are designed and operated to preclude the voiding condition in normally filled lines. The RCS and connecting accumulator lines including piping and components, are designed for normal, upset, emergency, and faulted condition transients. The design requirements are conservative relative to both the number of transients and their severity. Relief valve actuation and the associated hydraulic transients following valve opening are considered in the system design. Other valve and pump actuations are relatively slow transients with no significant effect on the system dynamic loads. To ensure dynamic system stability, reactor coolant parameters are stringently controlled. Temperature during normal operation is maintained within a narrow range by control rod position; pressure is controlled by pressurizer heaters and pressurizer spray also within a narrow range for steady-state conditions. The flow characteristics of the system remain

constant during a fuel cycle because the only governing parameters, namely system resistance and the reactor coolant pump characteristics are controlled in the design process. Additionally, Westinghouse has instrumented typical reactor coolant systems to verify the flow and vibration characteristics of the system and connecting accumulator lines. Preoperational testing and operating experience have verified the Westinghouse approach. The operating transients of the RCS primary piping and connected accumulator lines are such that no significant water hammer can occur.

3.3 Low Cycle and High Cycle Fatigue

Low cycle fatigue considerations are accounted for in the design of the piping system through the fatigue usage factor evaluation to show compliance with the rules of Section III of the ASME Code. A further evaluation of the low cycle fatigue loading is discussed in Chapter 7 as part of this study in the form of a fatigue crack growth analysis.

High cycle fatigue loads in the system would result primarily from pump vibrations during operation. During operation, an alarm signals the exceedance of the RC pump shaft vibration limits. Field measurements have been made on the reactor coolant loop piping of a number of plants during hot functional testing. Stresses in the elbow below the RC pump have been found to be very small, between 2 and 3 ksi at the highest. When translated to the connecting accumulator lines, these stresses are even lower, well below the fatigue endurance limit for the accumulator line material and would result in an applied stress intensity factor below the threshold for fatigue crack growth.

3.4 References

- 3-1 Investigation and Evaluation of Stress-Corrosion Cracking in Piping of Light Water Reactor Plants, NUREG-0531, U.S. Nuclear Regulatory Commission, February 1979.
- 3-2 Investigation and Evaluation of Cracking Incidents in Piping in Pressurized Water Reactors, NUREG-0691, U.S. Nuclear Regulatory Commission, September 1980.

SECTION 4.0

MATERIAL CHARACTERIZATION

4.1 Pipe, Fittings and Weld Materials

The pipe material of the 12-inch high energy accumulator lines is SA 376-TP316, a wrought product form of the type used for the primary loop piping of several PWR plants. The fittings are SA403-WP316 which is wrought and formed pipe of SA182 F316. The weld wire used in the shop fabrication is generally low carbon 316L; in some instances the weld wire has low carbon with high silicon (316LSi). The welding processes used were gas tungsten arc (GTAW), submerged arc (SAW), gas metal arc (GMAW) and shielded metal arc (SMAW). The field welds used 308L weld wire. For each line there is a 45 degree nozzle intersecting the cold leg of the primary loop. The material of these nozzles is SA351 CF8A, a cast product form.

In the following section the tensile and fracture toughness properties of these materials are presented and criteria for use in the leak-before-break analyses are defined.

4.2 Tensile Properties

The material certifications for the 12-inch high energy lines were used to establish the tensile properties for the piping, fittings and welds. The properties are given in Table 4-1 and 4-2 for Units 1 and 2, respectively. Tensile properties for the 45° cast nozzle are given in Table 4-3.

The properties in Table 4-1 through 4-3 are those at room temperature. In the leak-before-break evaluations presented later, the code minimum properties at operating temperatures are used. The viability of using such properties for the 12-inch high energy accumulator lines is presented below.

[

]a,c,e

[

] ^{a,c,e} All the properties presented are seen to exceed the code minimum properties. Larger margins are noted when comparing the experimental yield stress data with the code minimum properties.

Based on this discussion it is concluded that the use of code minimum properties is justified. [

] ^{a,c,e}

4.3 Fracture Toughness Properties

[

] ^{a,c,e}

Lower bound estimates for the fracture toughness of welds, taking thermal aging into account, are discussed in Reference 4-4. [

] ^{a,c,e}

Forged stainless steel is considered not susceptible to thermal aging for the applications at hand; however, thermal aging embrittlement must be considered for the cast 45° nozzle.

[

] ^{a,c,e} By the

criteria established in Reference 4-5, the fracture toughness is at least as great as the toughness of [] ^{a,c,e}.

[]^{a,c,e} is the same heat which serves as a lower bound for welds as seen in Table 4-6. [

] ^{a,c,e} The fracture criteria are

thus

[] ^{a,c,e}

4.4 References

- 4-1 F. J. Witt et al., "Integrity of the Primary Piping System of Westinghouse Nuclear Power Plants During Postulated Seismic Events," WCAP-9283, March 1978.
- 4-2 S. S. Palusamy, "Tensile and Toughness Properties of Primary Piping Weld Metal for Use in Mechanistic Fracture Evaluation," WCAP 9787, May, 1981 (Westinghouse Proprietary Class 2).
- 4-3 S. S. Palusamy, et al., "Mechanistic Fracture Evaluation of Reactor Coolant Pipe Containing a Postulated Circumferential Through-Wall Crack," WCAP-9558, Rev. 2, May 1982, (Westinghouse Proprietary Class 2).
- 4-4 W. H. Bamford, et al., "The Effects of Thermal Aging on the Structural Integrity of Cast Stainless Steel Piping for Westinghouse Nuclear Steam Supply Systems," WCAP-10456, November, 1983 (Westinghouse Proprietary Class 2).
- 4-5 F. J. Witt and C. C. Kim, "Toughness Criteria for Thermally Aged Cast Stainless Steel," WCAP 10931, Revision 1, July 1986 (Westinghouse Proprietary Class 2).

TABLE 4-1

ROOM TEMPERATURE MECHANICAL PROPERTIES
OF THE HIGH PRESSURE ACCUMULATOR LINE MATERIALS
AND WELDS OF THE SOUTH TEXAS PROJECT UNIT 1 PLANT

Loop No.	Product Form	Heat Number	Material	2% Offset Yield Stress	Ultimate Strength	Flow Stress	% Elongation Per Inch	% Reduction In Area
1	Pipe	HT P8608	SA376-TP316	43,300	85,600	64,450	58.5	71.7
1	Pipe	HT L5093	SA376-TP316	42,700	88,200	65,450	53.2	64.1
1	Pipe	HT L5091	SA376-TP316	38,100	82,600	60,350	60.5	71.2
1	Fitting	HT 55893	SA403-WP316	49,000	81,500	65,250	62.0	75.5
1	Fitting	HT 55896	SA403-WP316	50,000	82,000	66,000	56.0	73.5
1	Weld	HT 17138	SFA5.9-ER316L	67,200	83,600	75,400	50.0	65.5
1	Weld	HT 17138	SFA5.9-ER316L	65,400	88,700	77,050	48.0	65.9
1	Weld	HT 0575	SFA5.4-E316L	57,400	80,400	68,900	45.0	63.8

4-4

TABLE 4-1 (Continued)

ROOM TEMPERATURE MECHANICAL PROPERTIES
OF THE HIGH PRESSURE ACCUMULATOR LINE MATERIALS
AND WELDS OF THE SOUTH TEXAS PROJECT UNIT 1 PLANT

Loop No.	Product Form	Heat Number	Material	2% Offset Yield Stress	Ultimate Strength	Flow Stress	% Elongation Per Inch	% Reduction In Area
2	Pipe	HT P8608	SA376-TP316	43,300	85,600	64,450	58.5	71.7
2	Pipe	HT L5093	SA376-TP316	42,700	88,200	65,450	53.2	64.1
2	Pipe	HT L5091	SA376-TP316	38,100	82,600	60,350	60.5	71.2
2	Fitting	HT 55896	SA403-WP316	50,000	82,000	66,000	56	73.5
2	Fitting	HT 55894	SA403-WP316	50,500	79,000	64,750	45	70.5
2	Fitting	HT 55896	SA403-WP316	51,000	81,500	66,250	56.0	74.5
2	Weld	HT 17138	SFA5.9-ER316L	67,200	83,600	75,400	50.0	65.5
2	Weld	HT 17138	SFA5.9-ER316L	65,400	88,700	77,050	48.0	65.9
2	Weld	HT 0683A	SFA5.4-E316L	58,600	79,700	69,150	40.0	66.2

4-4

TABLE 4-1 (Continued)

ROOM TEMPERATURE MECHANICAL PROPERTIES
OF THE HIGH PRESSURE ACCUMULATOR LINE MATERIALS
AND WELDS OF THE SOUTH TEXAS PROJECT UNIT 1 PLANT

Loop No.	Product Form	Heat Number	Material	2% Offset Yield Stress	Ultimate Strength	Flow Stress	% Elongation Per Inch	% Reduction In Area
3	Pipe	HT L5093	SA376-TP316	40,100	83,000	61,550	59	67.9
3	Fitting	HT 55894	SA403-WP316	50,500	79,000	64,750	45	70.5
3	Weld	HT 306402	SFA5.9-ER316L	67,000	90,000	78,500	30.0	48.0
3	Weld	HT 19759	SFA5.9-ER316L	64,400	86,400	75,400	35.0	41.6

4-6

TABLE 4-2

ROOM TEMPERATURE MECHANICAL PROPERTIES
OF THE HIGH PRESSURE ACCUMULATOR LINE MATERIALS
AND WELDS OF THE SOUTH TEXAS PROJECT UNIT 2 PLANT

Loop No.	Product Form	Heat Number	Material	2% Offset Yield Stress	Ultimate Strength	Flow Stress	% Elongation Per Inch	% Reduction In Area
1	Pipe	HT L5091	SA376-TP316	38,100	82,600	60,350	60.5	71.2
1	Pipe	HT L5091	SA376-TP316	43,300	87,800	65,550	56.0	66.0
1	Pipe	HT L5091	SA376-TP316	44,100	88,600	66,350	52.0	67.3
1	Pipe	HT L5093	SA376-TP316	40,100	83,000	61,550	59.0	67.9
1	Pipe	HT L5093	SA376-TP316	40,500	84,600	62,550	59.5	68.2
1	Pipe	HT L5093	SA376-TP316	44,500	81,400	62,950	61	77.3
1	Fitting	HT 55895	SA403-WP316	51,000	81,500	66,250	56.0	74.5
1	Fitting	HT 53894	SA403-WP316	43,000	77,500	60,250	65	76.5
1	Fitting	HT 55893	SA403-WP316	49,000	81,500	65,250	62.0	75.0
1	Weld	HT 17138	SFA5.9-ER316L	67,200	83,600	75,400	50.0	65.5

4-7

TABLE 4-2 (Continued)

ROOM TEMPERATURE MECHANICAL PROPERTIES
OF THE HIGH PRESSURE ACCUMULATOR LINE MATERIALS
AND WELDS OF THE SOUTH TEXAS PROJECT UNIT 2 PLANT

Loop No.	Product Form	Heat Number	Material	2% Offset Yield Stress	Ultimate Strength	Flow Stress	% Elongation Per Inch	% Reduction In Area
1	Weld	HT 0575	SFA5.4-ER316L	57,400	80,400	68,900	45.0	63.8
1	Weld	HT 17138	SFA5.9-ER316L	62,600	86,700	74,650	36	65.4
2	Pipe	HT 1281-48	SA376-TP316	50,250	87,400	68,825	46	N/A
2	Pipe	HT 5-329	SA376-TP316	42,400	84,900	63,650	54	N/A
2	Pipe	HT L5736	SA376-TP316	42,100	89,000	65,550	62.3	66.4
2	Pipe	HT L5736	SA376-TP316	39,700	86,200	62,950	62.0	66.0
2	Pipe	HT L5093	SA376-TP316	44,500	81,400	62,900	61	77.3
2	Fitting	HT 989AN	SA403-WP316	43,400	83,800	63,600	64.7	81.0
2	Fitting	HT 102BN	SA403-WP316	43,100	82,800	62,950	59	81.0
2	Fitting	HT 53894	SA403-WP316	43,000	77,500	60,250	65.0	76.5

TABLE 4-2 (Continued)

ROOM TEMPERATURE MECHANICAL PROPERTIES
OF THE HIGH PRESSURE ACCUMULATOR LINE MATERIALS
AND WELDS OF THE SOUTH TEXAS PROJECT UNIT 2 PLANT

Loop No.	Product Form	Heat Number	Material	2% Offset Yield Stress	Ultimate Strength	Flow Stress	% Elongation Per Inch	% Reduction In Area
2	Fitting	HT 610AN	SA403-WP316	37,500	78,000	57,750	60	80.0
2	Weld	306402	SFA5.9-ER316L	67,000	90,000	78,500	30.0	48.0
2	Weld	2383B	SFA5.4-E316L	N/A	81,400	-	54.0	N/A
2	Weld	10300	SFA5.4-E316L	N/A	86,374	-	51.8	60.5
2	Weld	19759	SFA5.4-E316L	64,400	86,400	75,400	35.0	41.6
2	Weld	X-4329	SFA5.9-ER316L	70,600	92,500	81,550	38.0	59.6
3	Pipe	HT L5093	SA376-TP316	44,500	81,400	62,950	61	77.3
3	Fitting	HT 53894	SA403-WP316	43,000	77,500	60,250	65.0	76.5
3	Weld	306402	SFA5.9-ER316L	67,000	90,000	78,500	30.0	48.0
3	Weld	19759	SFA5.9-ER316L	64,400	86,400	75,400	35.0	41.6

4-9

TABLE 4-3

ROOM TEMPERATURE TENSILE PROPERTIES
OF THE SA351 CF8A CAST 45 DEGREE NOZZLE

<u>Unit</u>	<u>Loop</u>	<u>Yield Stress (ksi)</u>	<u>Ultimate Strength (ksi)</u>	<u>Elongation (%)</u>	<u>Reduction in Area %</u>
1	1	41.35	86.2	58	70
1	2	41.35	86.2	58	70
1	3	39.10	83.2	59	71
2	1	42.38	86.3	62	69
2	2	38.05	84.8	58	75
2	3	39.15	83.0	62	74

TABLE 4-4

TYPICAL TENSILE PROPERTIES OF SA376 TP316, SA351 CF8A and WELDS OF
SUCH MATERIAL FOR THE PRIMARY LOOP

Plant	Material	Test Temperature (°F)	Average Tensile Properties	
			Yield (psi)	Ultimate (psi)
A	SA376 TP316	70	40,900 (48) ^a	83,200 (48)
		650	23,500 (19)	67,900 (19)
	E 308 Weld	70	63,900 (3)	87,600 (3)
B	SA376 TP316	70	47,100 (40)	88,300 (40)
		650	26,900 (22)	69,100 (25)
	E 308 Weld	70	59,600 (8)	87,200 (8)
		650	31,500 (1)	68,800 (1)
C	SA376 TP316	70	46,600 (36)	87,300 (36)
		650	24,200 (18)	66,800 (19)
	E 308 Weld	70	61,900 (4)	85,400 (4)
D	SA351 CF8A	70	47,300 (14)	84,500 (14)
		650	26,000 (4)	70,500 (4)
	Weld	70	61,200 (31)	84,500 (32)

a. (____) indicates the number of test results averaged.

TABLE 4-5

COMPARISON OF TENSILE PROPERTIES OF THE 12-INCH
HIGH ENERGY ACCUMULATOR LINES WITH THOSE OF
TYPICAL WROUGHT PRIMARY LOOPS

Line/Component	Material	Properties (ksi)			
		Room Temperature		650°F	
		Yield	Ultimate	Yield	Ultimate
Acc/Pipe	SA376-TP316	38.1 to 50.3 ^a	81.4 to 89.0 ^a		
Loop/Pipe	SA376-TP316	40.9 to 47.1 ^b	83.2 to 88.3 ^b	23.5 to 26.9 ^a	67.9 to 69.1 ^b
Acc/Fitting	SA403-TP316	37.5 to 51.0 ^a	77.5 to 83.8 ^a		
Acc/Nozzle	SA351-CF8A	38.1 to 42.4 ^a	83.0 to 86.2 ^a		
Loop/Pipe	SA351-CF8A	47.3 ^b	84.5 ^b	26.0 ^b	70.5 ^b
Acc/Weld	E316L, E316 LSi	57.4 to 67.2 ^a	79.7 to 90 ^a		
Loop/Weld	E308	59.9 to 63.9 ^b	85.4 to 87.6 ^b	31.5	68.8
Loop/Weld	E316			54.0 ^c	67.6 ^c

ASME Code Minimum Requirements

Pipe	SA376 TP316	30.0	75.0	17.9 to 18.5 ^d	64.5 to 71.8 ^d
Fittings	SA403-WP316	30.0	75.0	17.9 to 18.5 ^d	64.5 to 71.8 ^d
Fitting	SA351-CF8A	35.0	77.0	21.0	65.2
Welds	E316L, E316LSi		70.0		
Welds	E308		80.0		
Welds	E308L		75.0		

- a. Range of material certification data
b. Range of averages or average
c. The results are for 600°F
d. Depending on edition of ASME Code

TABLE 4-6

FRACTURE TOUGHNESS PROPERTIES TYPICAL OF THE SURGE LINE

Material	Test Temp. (°F)	Tensile Properties (psi)		J_{Ic} (in-lb/in ²)	T_{mat}
		Yield	Ultimate		
SA376 TP316	600	21,700	65,500	[] a,c,e
SA376 TP316	600	20,500	60,100		
Weld _f (E308 and E316)	600	45,000 ^b	61,200 ^b		
Weld _f	600	--	--		
SA251 CF8A ^h	600	--	--		

4-13

[
b. Lowest of 6 tests.

] a,c,e

] a,c,e

TABLE 4-7

CHEMISTRY AND ENDS OF SERVICE LIFE RCU TOUGHNESS
FOR THE SIX 45° NOZZLES

a, c, e

SECTION 5.0

LOADS FOR FRACTURE MECHANICS ANALYSIS

Figures 5-1, 5-2 and 5-3 show schematic layout of the three accumulator lines. Note that only the high pressure region is included in the scope of this work.

The stresses due to axial loads and bending moments were calculated by the following equation:

$$\sigma = \frac{F}{A} + \frac{M}{Z} \quad (5.1)$$

where,

- σ = stress
- F = axial load
- M = bending moment
- A = metal cross-sectional area
- Z = section modulus

The bending moments for the desired loading combinations were calculated by the following equation:

$$M = \sqrt{M_Y^2 + M_Z^2} \quad (5.2)$$

where,

- M = bending moment for required loading
- M_Y = Y component of bending moment
- M_Z = Z component of bending moment

The axial load and bending moments for crack stability analysis and leak rate predictions were computed by the methods explained in Sections 5.1 and 5.2.

5.1 Loads for Crack Stability Analysis

The faulted loads for the crack stability analysis were calculated by the following equations:

$$F = |F_{DW} + F_{TH1} + F_p| + |F_{SSE}| \quad (5.3)$$

$$M_Y = |(M_Y)_{DW} + (M_Y)_{TH1}| + |(M_Y)_{SSE}| \quad (5.4)$$

$$M_Z = |(M_Z)_{DW} + (M_Z)_{TH1}| + |(M_Z)_{SSE}| \quad (5.5)$$

Where, the subscripts of the above equations represent the following loading cases,

DW = deadweight

TH1 = maximum thermal expansion including applicable thermal anchor motion

SSE = SSE loading including seismic anchor motion

P = load due to internal pressure

5.2 Loads for Leak Rate Evaluation

The normal operating loads for leak rate predictions were calculated by the following equations:

$$F = F_{DW} + F_{TH2} + F_p \quad (5.6)$$

$$M_Y = (M_Y)_{DW} + (M_Y)_{TH2} \quad (5.7)$$

$$M_Z = (M_Z)_{DW} + (M_Z)_{TH2} \quad (5.8)$$

Where, the subscript TH2 represents normal operating thermal expansion loading. All other parameters and subscripts are the same as those explained in Section 5.1.

5.4 Summary of Loads, Geometry and Materials

Table 5-1 provides a summary of envelope loads computed for fracture mechanics evaluations in accordance with the methods described in Section 5.1, 5.2 and 5.3. The cross-sectional dimensions and materials are also summarized. Load data is tabulated at the [

components are provided in Table 5-2. [

]a,c,e The loading

]a,c,e

TABLE 5-1
SUMMARY OF ENVELOPE LOADS

LOCATION	CONDITION	NODE NO	LOOP	MATERIAL	OUTSIDE DIA (inches)	SCHEDULE	NOMINAL WALL THICK (inches)	MINIMUM WALL THICK (inches)	INSIDE DIA (inches)	F (kips)	M (in-kips)
Highest Load Location	Faulted	104E	1	SA376 -TP316	12.75	140	1.125	1.005	10.74	194	1006
	Normal Operating	104E	1	SA376 -TP316	12.75	140	1.125	1.005	10.74	193	978.2
Next Highest Load Location	Faulted	796	3	SA376 -TP316	12.75	140	1.125	1.005	10.74	200	975
	Normal Operating	796	3	SA376 -TP316	12.75	140	1.125	1.005	10.74	197	610.5

5-4

TABLE 5-2
LOADING COMPONENTS AT GOVERNING LOCATIONS

Load Type	Highest Load (Location - 104E, Loop-1)			Next Highest Load (Location - 796, Loop-3)		
	Axial Force (lb)	Bending Moment MY (ft-lb)	Bending Moment MZ (ft-lb)	Axial Force (lb)	Bending Moment MY (ft-lb)	Bending Moment MZ (ft-lb)
Dead Weight	279	55	3867	-615	1785	2422
Thermal	-6521	612	77649	-1913	15583	-50244
Pressure	199526	-	-	199526	-	-
SSE + Anch. Mot.	709	2833	2266	3013	25520	21179

5-5

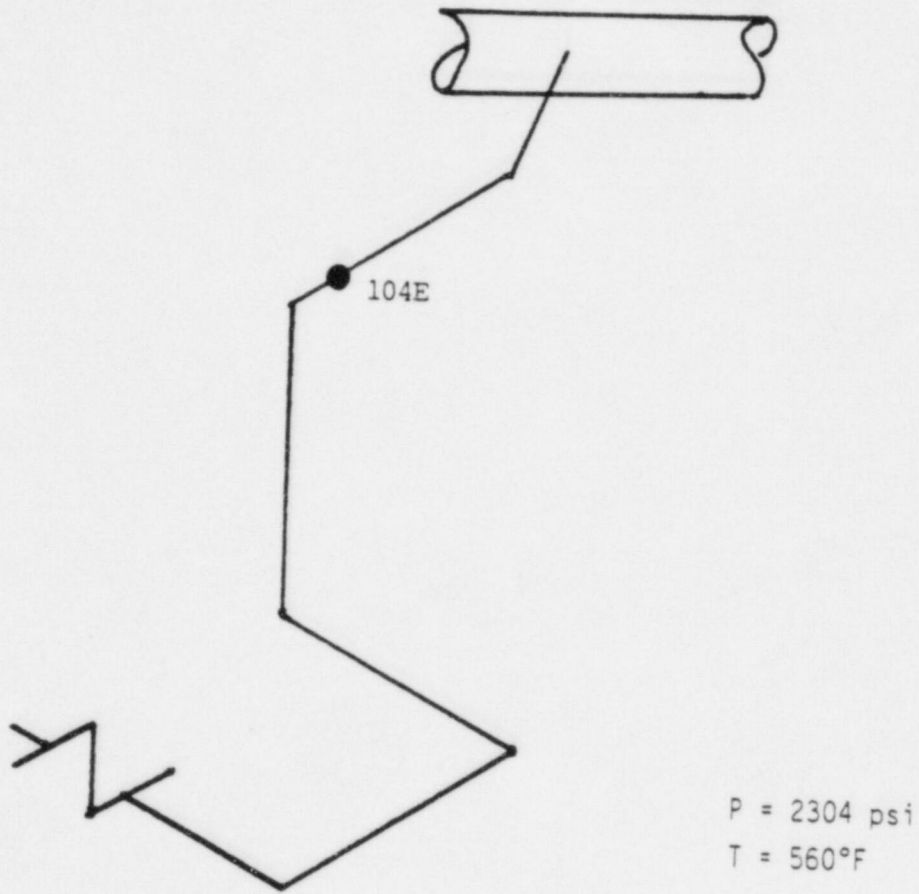
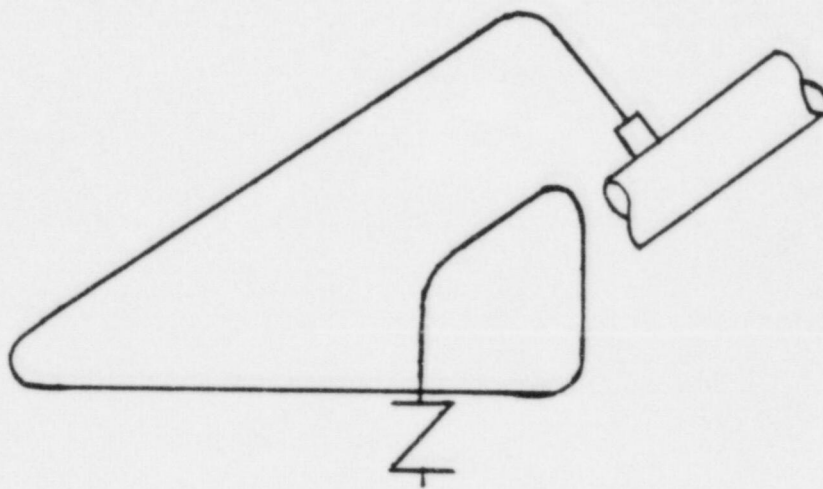
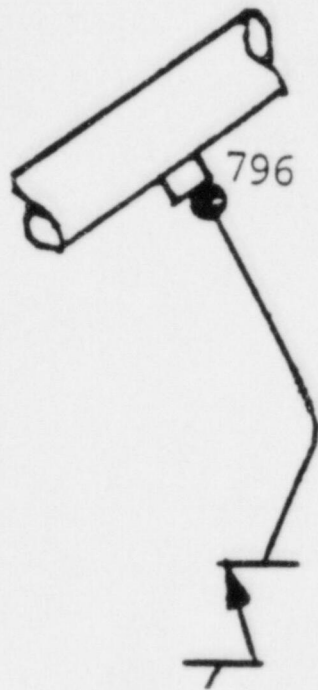


Figure 5-1: Schematic Layout of Accumulator Line Loop 1



P = 2304 psi
T = 560°F

Figure 5-2: Schematic Layout of Accumulator Line Loop 2



P = 2304 psi
T = 560°F

Figure 5-3: Schematic Layout of Accumulator Lines Loop 3

SECTION 6.0

FRACTURE MECHANICS EVALUATION

6.1 Global Failure Mechanism

Determination of the conditions which lead to failure in stainless steel should be done with plastic fracture methodology because of the large amount of deformation accompanying fracture. One method for predicting the failure of ductile material is the plastic instability method, based on traditional plastic limit load concepts, but accounting for strain hardening and taking into account the presence of a flaw. The flawed pipe is predicted to fail when the remaining net section reaches a stress level at which a plastic hinge is formed. The stress level at which this occurs is termed as the flow stress. The flow stress is generally taken as the average of the yield and ultimate tensile strength of the material at the temperature of interest. This methodology has been shown to be applicable to ductile piping through a large number of experiments and will be used here to predict the critical flaw size in the accumulator line. The failure criterion has been obtained by requiring equilibrium of the section containing the flaw (Figure 6-1) when loads are applied. The detailed development is provided in Appendix A for a through-wall circumferential flaw in a pipe with internal pressure, axial force, and imposed bending moments. The limit moment for such a pipe is given by:

$$[\quad] \quad a,c,e \quad (6.1)$$

where:

$$[\quad] \quad a,c,e$$

[

$$j^{a,c,e} \quad (6.2)$$

The analytical model described above accurately accounts for the piping internal pressure as well as imposed axial force as they affect the limit moment. Good agreement was found between the analytical predictions and the experimental results (Reference 6-1).

A typical segment of the accumulator pipe under maximum loads of axial force F and bending moment M is schematically illustrated as shown in Figure 6-2. In order to calculate the critical flaw size, a plot of the limit moment versus crack length is generated as shown in Figure 6-3. The critical flaw size corresponds to the intersection of this curve and the maximum load line.

The critical flaw size is calculated to be [$j^{a,c,e}$] using ASME Code (6-2) minimum tensile properties for SA376TP316 (wrought) stainless steel. [$j^{a,c,e}$]

Since $W_p > 1006$ in-kips for cracks smaller than [$j^{a,c,e}$] and $W_a = 1006$ in-kips, the global stability criterion of Section 2.2 is satisfied.

If IWB 3640 approach is used and if the material strength properties are conservatively assumed to be the same as the base metal properties, the critical flaw size for the weld metal would be about [$j^{a,c,e}$]

6.2 Leak Rate Predictions

Fracture mechanics analysis shows that postulated through-wall cracks in the accumulator line would remain stable and not cause a gross failure of this component. If such a through-wall crack did exist, it would be desirable to detect the leakage such that the plant could be brought to a safe shutdown condition. The purpose of this section is to discuss the method which will be used to predict the flow through such a postulated crack and present the leak rate calculation results for through-wall circumferential cracks.

6.2.1 General Considerations

The flow of hot pressurized water through an opening to a lower back pressure causes flashing which can result in choking. For long channels where the ratio of the channel length, L , to hydraulic diameter, D_H , (L/D_H) is greater than $[]^{a,c,e}$, both $[]^{a,c,e}$ must be considered. In this situation the flow can be described as being single-phase through the channel until the local pressure equals the saturation pressure of the fluid. At this point, the flow begins to flash and choking occurs. Pressure losses due to momentum changes will dominate for $[]^{a,c,e}$. However, for large L/D_H values, friction pressure drop will become important and must be considered along with the momentum losses due to flashing.

6.2.2 Calculation Method

The basic method used in the leak rate calculations is the method developed by [

$]^{a,c,e}$

The flow rate through a crack was calculated in the following manner. Figure 6-4 from Reference 6-3 was used to estimate the critical pressure, P_c , for the accum. line enthalpy condition and an assumed flow. Once P_c was found for a given mass flow, the $[]^{a,c,e}$ was found from Figure 6-5 taken from Reference 6-3. For all cases considered, since $[]^{a,c,e}$ Therefore, this method will yield

the two-phase pressure drop due to momentum effects as illustrated in Figure 6-6. Now using the assumed flow rate, G, the frictional pressure drop can be calculated using

$$\Delta P_f = [\dots]^{a,c,e} \quad (6.3)$$

where the friction factor f is determined using the [\dots]^{a,c,e}. The crack relative roughness, ε, was obtained from fatigue crack data on stainless steel samples. The relative roughness value used in these calculations was [\dots]^{a,c,e} RMS.

The frictional pressure drop using Equation 6.3 is then calculated for the assumed flow and added to the [momentum pressure drop calculated using the Fauske model]^{a,c,e} to obtain the total pressure drop from the primary system to the atmosphere. That is, for the primary loop

$$\text{Absolute Pressure} - 14.7 = [\dots]^{a,c,e} \quad (6.4)$$

for a given assumed flow G. If the right-hand side of Equation 6.4 does not agree with the pressure difference between the accumulator line and the atmosphere, then the procedure is repeated until Equation 6.4 is satisfied to within an acceptable tolerance and this results in the flow value through the crack. This calculational procedure has been recommended by [\dots]^{a,c,e} for this type of [\dots]^{a,c,e} calculation.

6.2.3 Leak Rate Calculations

Leak rate calculations were made as a function of postulated through-wall crack length for the critical location previously identified. The crack opening area was estimated using the method of Reference 6-5 and the leak rate was calculated using the two-phase flow formulation described above. The leak

rates are calculated using the normal operating loads of axial force, $F = 193$ kips and bending moment, $M = 978$ in-kips. The leak rates for various postulated crack lengths are shown in Figure 6-7. In this figure, the crack length yielding, a leak rate of 10 gpm (10 times the leak detection capability of 1 gpm per Reg. Guide 1.45) is found to be []^{a,c,e} long. Thus, the "reference" flaw size of []^{a,c,e} is established.

6.3 Local Failure Mechanism

In this section the local stability analysis is performed to show that unstable crack extension will not result for a flaw two times as long as the "reference" flaw.

At the critical location, the outer surface axial stress, σ_a , is seen to be 15.2 ksi. Circumferential and radial stresses due to internal pressure of 2304 psi are as follows (see Reference 6-6):

σ_c (circumferential stress): 11.26 ksi

σ_r radial stress: 0

The von Mises effective stress, σ_{eff} , (see Reference 6-7) is given by

$$\sigma_{eff} = \frac{1}{\sqrt{2}} \sqrt{(\sigma_a - \sigma_r)^2 + (\sigma_c - \sigma_r)^2 + (\sigma_a - \sigma_c)^2}$$

and is 13.7 ksi.

Thus the effective stress is less than the yield stress and by the Von Mises plasticity theory yielding does not occur. Hence, linear elastic fracture mechanics is applicable for analyzing the pipes with hypothesized flaws. The analytical method used for the local stability evaluation at this location is summarized below.

The stress intensity factors corresponding to tension and bending are expressed, respectively, by (see Reference 6-5)

$$K_t = \sigma_t \sqrt{\pi a} F_t(\alpha)$$

$$K_b = \sigma_b \sqrt{\pi a} F_b(\alpha)$$

where $F_t(\alpha)$ and $F_b(\alpha)$ are stress intensity calibration factors corresponding to tension and bending, respectively, a is the half-crack length, α is the half-crack angle, σ_t is the remote uniform tensile stress, and σ_b is the remote fiber stress due to pure bending. Data for $F_t(\alpha)$ and $F_b(\alpha)$ are given in Reference 6-5. The effect of the yielding near the crack tip can be incorporated by Irwin's plastic zone correction method (see Reference 6-8) in which the half-crack length, a , in these formulas is replaced by the effective crack length, a_{eff} , defined by

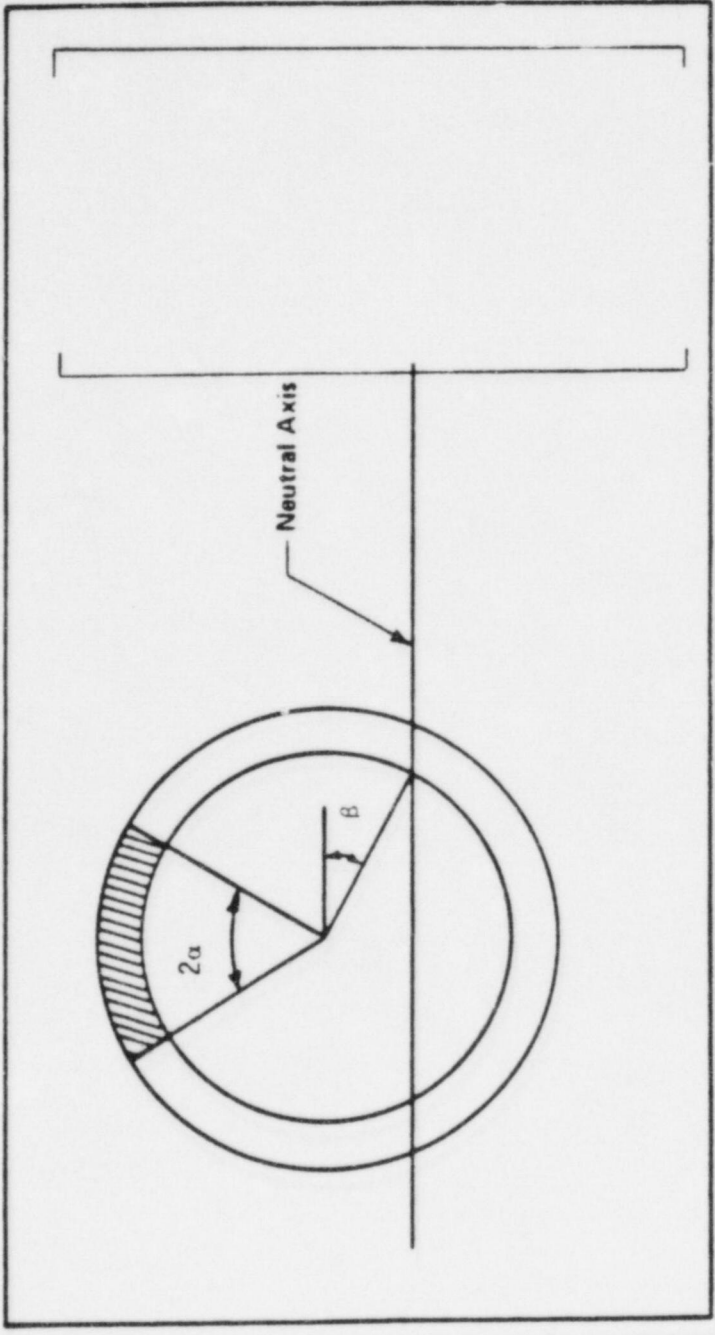
$$a_{eff} = a + \frac{1}{2\pi} \frac{K^2}{\sigma_y^2}$$

for plane stress plastic corrections, where σ_y is the yield strength of the material and K is the total stress intensity factor due to combined tensile and bending loads (i.e., $K = K_t + K_b$). Finally, the J_{app} -value is determined by the relation $J_{app} = K^2/E$, where E is Young's Modulus.

J_{app} was calculated for a []^{a,c,e} long postulated through-wall crack (which is 2 times the reference flaw size) and was found to be []^{a,c,e}. In addition, for a leakage size flaw i.e. the reference flaw of []^{a,c,e} long the normal plus SSE load was increased by $\sqrt{2}$. The J-T analysis gave an applied J of []^{a,c,e}. Clearly, the applied J is lower than J_{Ic} of []^{a,c,e} for both the above cases and hence no unstable crack propagation will not result.

6.4 Reference

- 6-1 Kanninen, M. F. et al., "Mechanical Fracture Predictions for Sensitized Stainless Steel Piping with Circumferential Cracks" EPRI NP-192, September 1976.
- 6-2 ASME Section III, Division 1-Appendices, 1986 Edition, July 1, 1986.
- 6-3 []
]a,c,e
- 6-4 []
]a,c,e.
- 6-5 Tada, H., "The Effects of Shell Corrections on Stress Intensity Factors and the Crack Opening Area of Circumferential and a Longitudinal Through-Crack in a Pipe," Section II-1, NUREG/CR-3464, September 1983.
- 6-6 Durelli, A. J., et. al., Introduction to the Theoretical and Experimental Analysis of Stress and Strain, McGraw Hill Book Company, New York, (1958), pp. 233-236.
- 6-7 Johnson, W. and Mellor, P. B., Engineering Plasticity, Van Nostrand Reinhold Company, New York, (1973), pp. 83-86.
- 6-8 Irwin, G. R., "Plastic Zone Near a Crack and Fracture Toughness," Proc. 7th Sagamore Conference, P. IV-63 (1960).

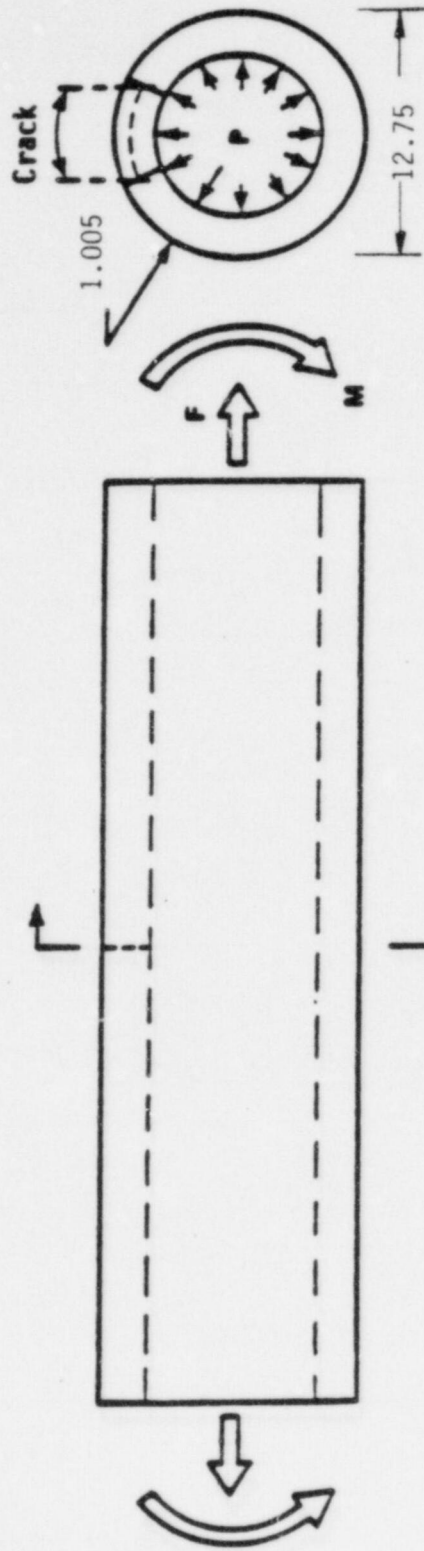


a, c, e

a, c, e

] stress distribution

Figure 6-1 [

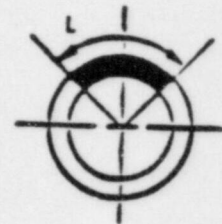


] a, c, e

[

Figure 6-2 Loads Acting on the Pipe Model

a, c, e



FLAW GEOMETRY

OD = 12.75"
t = 1.005"
P = 2304 psig
F = 194 kips
 $\sigma_y = 19.2$ ksi
 $\sigma_u = 71.8$ ksi
 $\sigma_F = 45.5$ ksi
Temp = 560°F

Figure 6-3 "Critical" Flaw Size Prediction

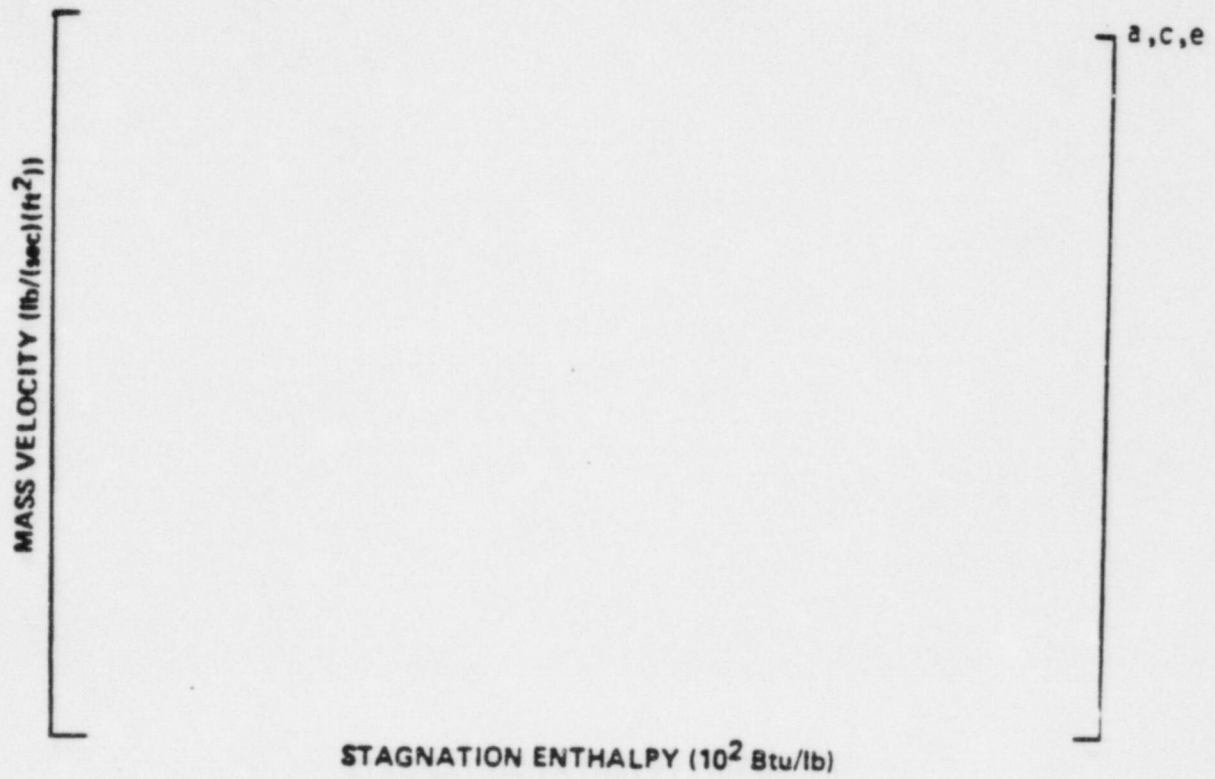


Figure 6-4 Analytical Predictions of Critical Flow Rates of Steam-Water Mixtures

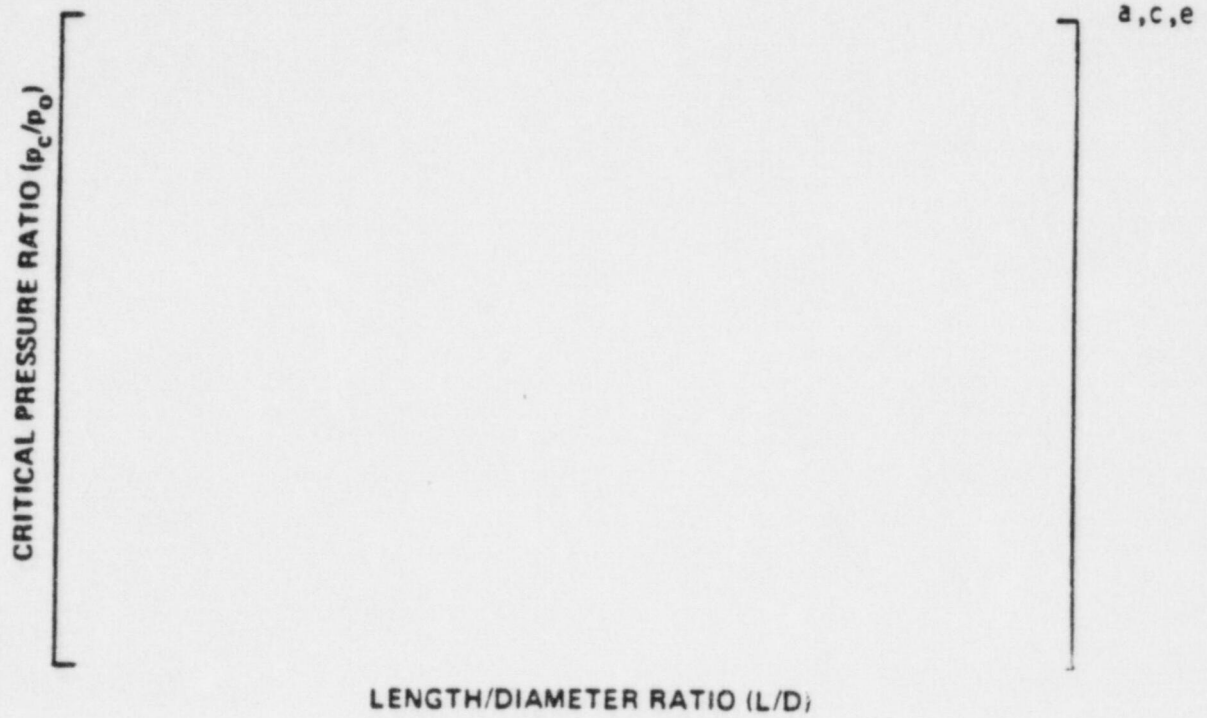


Figure 6-5

$]^{a,c,e}$ Pressure Ratio as a Function of L/D

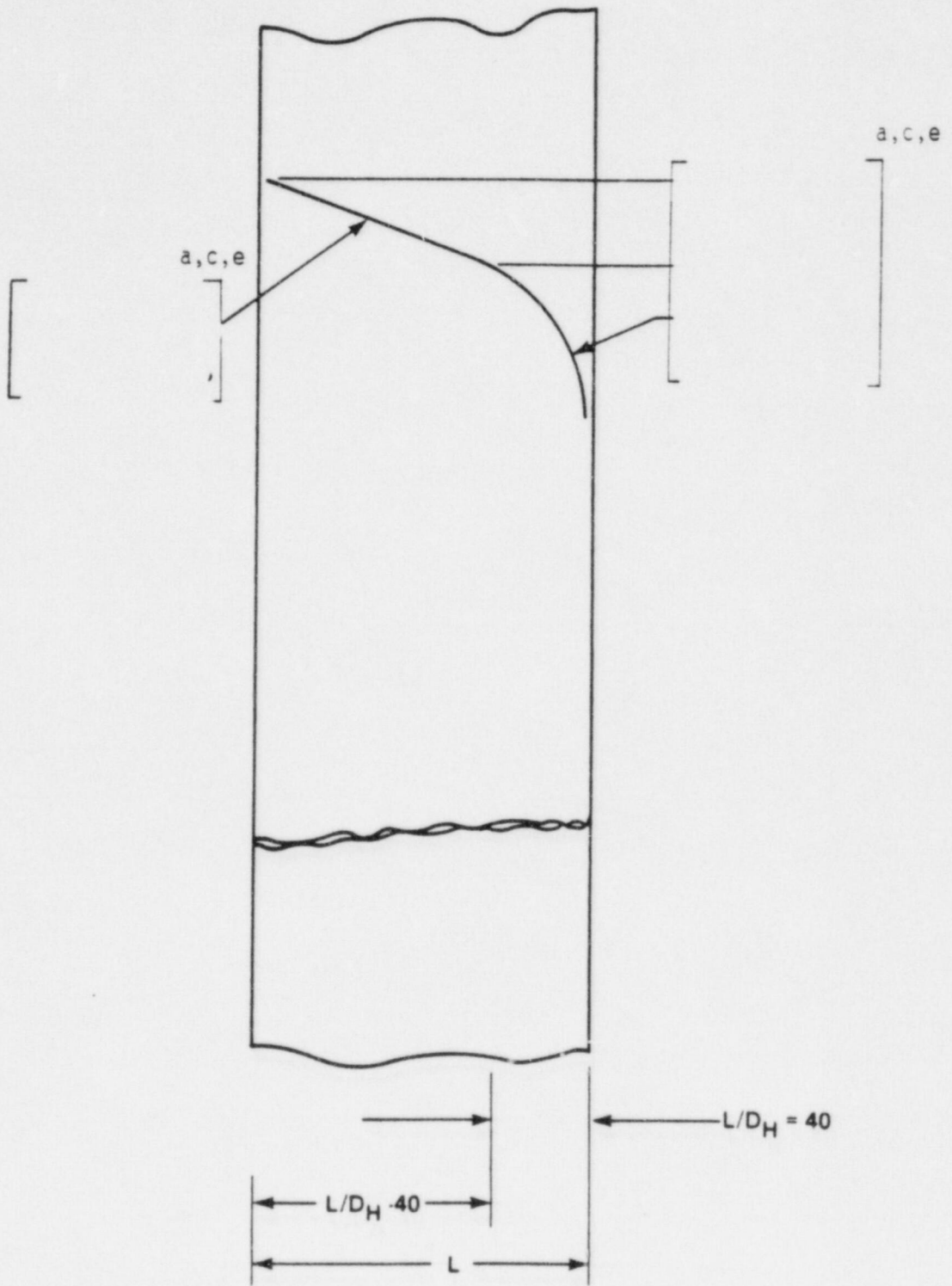


Figure 6-6 Idealized Pressure Drop Profile Through a Postulated Crack

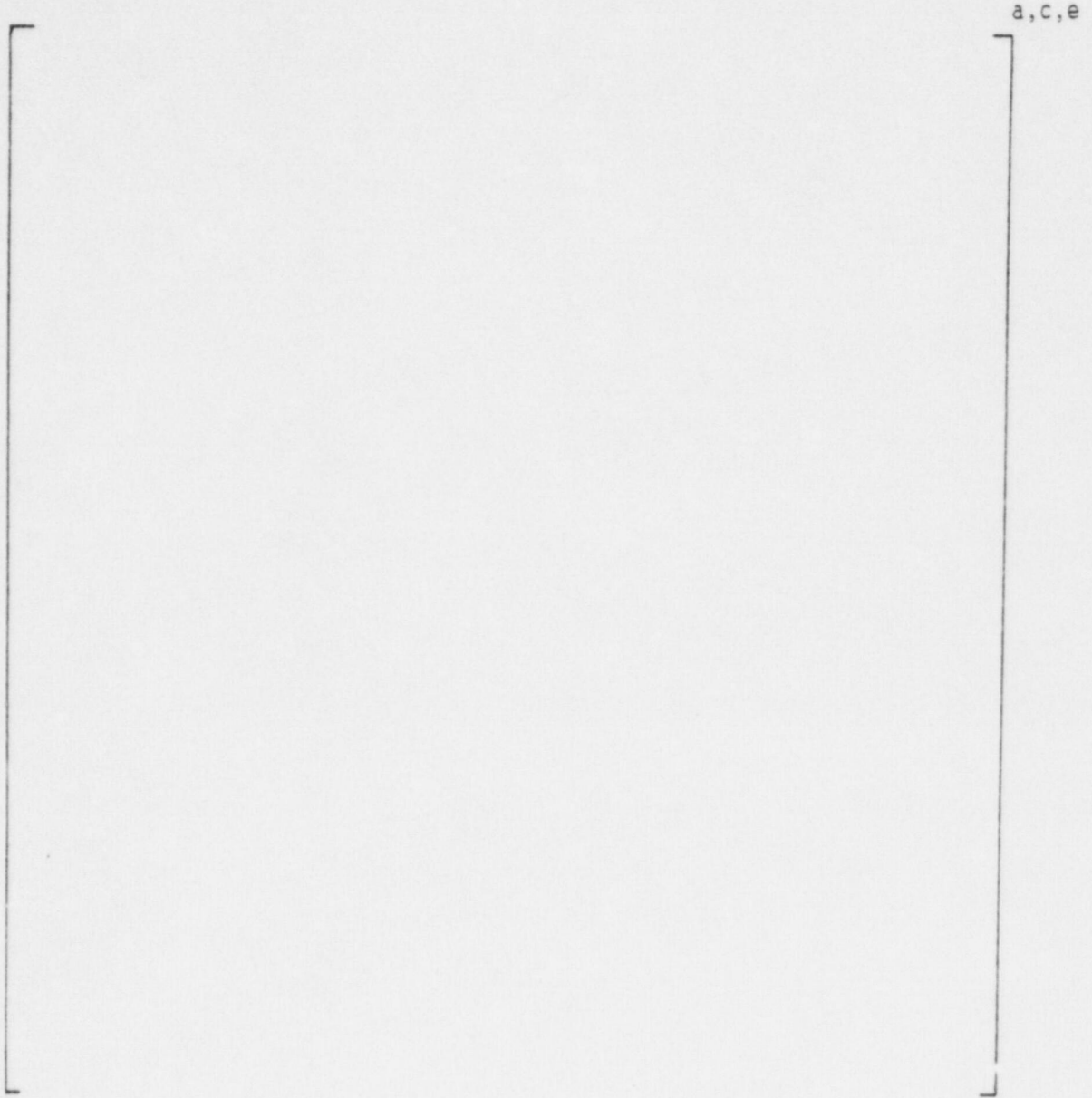


Figure 6-7 Leak Rate Versus Crack Length

SECTION 7.0

ASSESSMENT OF FATIGUE CRACK GROWTH

The fatigue crack growth on the South Texas accumulator line was determined by comparison with a generic fatigue crack growth analysis of a similar piping system. The details of the generic fatigue crack growth analysis are presented in Appendix B. By comparing all parameters critical to the fatigue crack growth analysis, between South Texas and generic, it was concluded that the generic analysis would envelop the fatigue crack growth of the South Texas accumulator line.

Due to similarities in Westinghouse PWR designs it was possible to perform a generic fatigue crack growth calculation which would be applicable to many projects. A comparison was made of stresses and number of cycles, material, geometry, and types of discontinuities.

A review of all thermal transient and steady-state stresses indicated a significant margin in the generic analysis. This was caused primarily by a reduced number of safety injection transients for South Texas because of the 4XL design. Geometry was essentially identical with the South Texas pipe being 12 inch schedule 140 versus the generic of 10 inch schedule 140. Both generic and South Texas had the same materials for the piping, SA376-TP316 austenitic stainless steel. Although the nozzle materials are slightly different, SA-351-CF8A versus SA-182-304N or SA-182-316N for the generic case, the lower yield strength of the piping was still controlling.

In conclusion, the fatigue crack growth calculated for the generic case, as summarized in section B.2.2, is applicable to the South Texas accumulator lines. These results demonstrate that no significant fatigue crack growth will occur over the 40 year plant design life even for the largest postulated flaw.

7.1 Acceptability Fatigue Crack Growth

A detailed discussion pertaining to the fatigue crack growth law used in the analysis described in Appendix B and the data used in defining the law are provided in Reference (7-1). For the assessment of crack growth acceptability, the crack growth results of the generic analysis presented in Appendix B are used conservatively and are considered applicable to the South Texas Project Accumulator lines. Detailed discussion in support of this assumption has been provided in the previous section.

The maximum allowable preservice indication may have a depth of 0.09 in. per IWB-3514.3, Allowable Indication Standard for Austenitic Piping, ASME Code, Section XI - Division 1, 1986 edition. Typical fatigue crack growth results for various initial flaw depths are given in Table B-4 in the appendix to this report. [

] a,c,e is

conservatively chosen as a basis for examining the NRC criteria (7-1) pertaining to allowable fatigue crack growth. [

] a,c,e

Thus, the first criterion on flaw depth is satisfied.

The worst case transient ΔK value for the maximum crack depth is [] a,c,e
The flow stress for the base metal at 560°F is 45.5 ksi which can be used to obtain a conservative estimate of the plastic zone size.

The expression for plastic zone size, r_p , calculation is: [] a,c,e

$$r_p = \frac{\pi}{32} \left(\frac{\Delta K}{\sigma_{\text{flow}}} \right)^2$$

Thus, the plastic zone size is calculated to be [] a,c,e The remaining ligament for the 0.186 in. deep end-of-fatigue-life flaw is 0.819 in. (i.e. 1.005 - 0.186). Thus, the plastic zone size is less than the remaining ligament.

Based on the above, it is concluded that for the South Texas Project Accumulator Lines, the fatigue crack growth during service will not be significant.

7.2 References

- 7-1 Swamy, S.A., et. al., "Additional Information in Support of the Elimination of Postulated Pipe Ruptures in the Pressurizer Surge Lines of South Texas Project Units 1 and 2" WCAP-11256, September 1986, (Westinghouse Proprietary Class 2).

- 7-2 Swamy, S. A., et. al., "Technical Bases for Eliminating Pressurizer Surge Line Ruptures as the Structural Design Basis for South Texas Project Units 1 and 2" WCAP-11256 Supplement 1, November 1986 (Westinghouse Proprietary Class 2).

SECTION 8.0

ASSESSMENT OF MARGINS

In the preceding sections, the leak rate calculations, fracture mechanics analysis and fatigue crack growth assessments were performed. Margins are discussed below.

As shown in Section 5.4 the maximum axial stress at the outside surface of the pipe is only 15.2 ksi. The ASME Code minimum yield strength at normal operating temperature is 19.2 ksi. Thus the maximum faulted condition axial stress including deadweight, thermal, pressure and SSE loads is less than 80 percent of the yield strength of the material.

In Section 6.1, the critical flaw size using limit load methods is calculated to be []^{a,c,e}. If IWB-3640 approach is used the critical flaw size for the weld metal would be about []^{a,c,e}. In Section 6.3 it is seen that the J value at maximum load is []^{a,c,e} for a []^{a,c,e} long postulated through-wall flaw. This J value is significantly lower than the lower bound J_{Ic} value of []^{a,c,e} considering thermal aging effects. The flaw size yielding a J value of []^{a,c,e} would be about []^{a,c,e} long. Based on the above, the critical flaw size will, of course, exceed []^{a,c,e}.

In Section 6.2 it is shown that at the critical location, a flaw of []^{a,c,e} would yield a leak rate of 10 gpm. Thus, there is a margin of at least 2.5 on flaw size.

In Section 6.3 it was shown that the reference flaw []^{a,c,e} yielding a leak rate of 10 gpm would be stable when subjected to a load equal to $\sqrt{2}$ (Normal + SSE).

In summary, relative to:

1. Loads

- a. Maximum stress at the critical location is less than 80 percent of the ASME code minimum yield strength at temperature.
- b. The leakage-size crack will not experience unstable crack extension even if larger loads of $\sqrt{2}$ (normal plus SSE) are applied.

2. Flaw Size

- a. A margin of at least 2.5 exists between the critical flaw and the flaw yielding a leak rate of 10 gpm.
- b. If limit load is used as the basis for critical flaw size the margin for global stability would exceed 4.

3. Leak Rate

A margin of 10 exists for the reference flaw []^{a,c,e}
between calculated leak rate and the criteria of Regulatory Guide 1.4.5.

A summary comparison of criteria and analytical results is given in Table 8-1. The criteria are seen to be met.

TABLE 8-1
COMPARISON OF RESULTS VS. CRITERIA

<u>CRITERION</u>	<u>RESULT</u>
1. NUREG1061 Volume 3 Section 5.2(h) - Margin on Flaw Size	Met (Required margin of 2 demonstrated)
2. NUREG1061 Volume 3 Section 5.2(i) - Margin on Load	Met (Required margin of $\sqrt{2}$ demonstrated)
3. NUREG 1061 Volume 3 Section 5.7 - Margin on Leak Rate	Met (Required margin of 10 on leak rate demonstrated)
4. NRC criteria on allowable fatigue crack growth ($a_f < 60\%$ wall thickness)	Met [] ^{a,c,e}
5. NRC criteria on allowable fatigue crack growth (Plastic zone size < remaining ligament)	Met [] ^{a,c,e}

SECTION 9.0

CONCLUSIONS

This report justifies the elimination of Accumulator line pipe breaks (high pressure segment) for the South Texas Project Units 1 and 2 as follows:

- a. Stress corrosion cracking is precluded by use of fracture resistant materials in the piping system and controls on reactor coolant chemistry, temperature, pressure, and flow during normal operation.
- b. Water hammer should not occur in the RCS piping (primary loop and the attached class 1 auxiliary lines) because of system design, testing, and operational considerations.
- c. The effects of low and high cycle fatigue on the integrity of the accumulator line piping are negligible.
- d. Ample margin exists between the leak rate of small stable flaws and the criterion of Reg. Guide 1.45.
- e. Ample margin exists between the small stable flaw sizes of item d and the critical flaw.
- f. Ample margin exists in the material properties used to demonstrate end-of-service life (relative to aging) stability of the critical flaws.
- g. With respect to stability of the reference flaw, ample margin exists between the maximum postulated loads and the plant specific faulted loads (i.e. Normal + SSE).

The reference flaw will be stable throughout reactor life because of the ample margins in d, e, f and g and will leak at a detectable rate which will assure a safe plant shutdown.

Based on the above, it is concluded that Accumulator line (high pressure segment) pipe breaks should not be considered in the structural design basis of South Texas Project Units 1 and 2.

APPENDIX A

LIMIT MOMENT

APPENDIX A

LIMIT MOMENT

[

] a,c,e



FIGURE A-1 PIPE WITH A THROUGH-WALL CRACK IN BENDING

APPENDIX B

FATIGUE CRACK GROWTH CONSIDERATIONS

B.1 Thermal Transient Stress Analysis

The thermal transient stress analysis was performed for a typical PWR plant to obtain the through wall stress profiles for use in the fatigue crack growth analysis of Section B.2. The through wall stress distribution for each transient was calculated for i) the time corresponding to the maximum inside surface stress and, ii) the time corresponding to the minimum inside surface stress. These two stress profiles are called the maximum and minimum through wall stress distribution, respectively for convenience. The constant stresses due to pressure, deadweight and thermal expansion (at normal operating temperature, 550°F) loadings were superimposed on the through wall cyclical stresses to obtain the total maximum and minimum stress profile for each transient. Linear through wall stress distributions were calculated by conservative simplified methods for all minor transients. More accurate nonlinear through wall stress distributions were developed for severe transients by []^{a,c,e}

B.1.1 Critical Location for Fatigue Crack Growth Analysis

The accumulator line stress report design thermal transients (Section B.1.2), 1-D analysis data on accumulator line thermal transient stresses (based on ASME Section III NB3600 rules) and the geometry were reviewed to select the worst location for the fatigue crack growth analysis. []

[]^{a,c,e} This location is selected as the worst location based on the following considerations:

- i) the fatigue usage factor is highest.
- ii) the stress due to thermal expansion is high.
- iii) the effect of discontinuity due to undercut at weld will tend to increase the cyclical thermal transient loads.
- iv) the review of data shows that the 1-D thermal transient stresses in the accumulator line piping section are generally higher near the []^{a,c,e}

B.1.2 Design Transients

The transient conditions selected for this evaluation are based on conservative estimates of the magnitude and the frequency of the temperature fluctuations resulting from various operating conditions in the plant. These are representative of the conditions which are considered to occur during plant operation. The fatigue evaluation based on these transients provides confidence that the component is appropriate for its application over the design life of the plant. All the normal operating and upset thermal transients, in accordance with design specification and the applicable system design criteria document (B-1), were considered for this evaluation. Out of these, only [

] ^{a,c,e} These transients were selected on the basis of the following criteria:

$$\left[\begin{array}{c} \dots \\ \dots \end{array} \right] \quad \begin{array}{l} \text{+a,c,e} \\ \text{(B.1)} \\ \text{(B.2)} \end{array}$$

where,

$$\left[\begin{array}{c} - \\ \dots \end{array} \right] \quad \text{+a,c,e}$$

B.1.3 Simplified Stress Analysis

The simplified analysis method was used to develop conservative maximum and minimum linear through wall stress distributions due to thermal transients. [

] ^{a,c,e} The inside surface stress was calculated by the following equation which is similar to the transient portion of ASME Section III NB3600, Eq. 11:

$$S_i = [\dots] \quad \text{+a,c,e} \quad \text{(B.3)}$$

where,

$$\left[\begin{array}{c} \dots \\ \dots \\ \dots \end{array} \right]^{a,c,e}$$

The material properties for the accumulator pipe [

$]^{a,c,e}$ The values of E and α , at the normal operating temperature, provide a conservative estimation of the through wall thermal transient stresses as compared to room temperature properties. The following values were conservatively used, which represent the highest of the [piping and nozzle] materials:

$$\left[\begin{array}{c} \dots \\ \dots \\ \dots \end{array} \right]^{a,c,e}$$

The maximum and minimum linear through wall stress distribution for each thermal transient was obtained by [

$]^{a,c,e}$ The simplified analysis discussed in this section was performed for all minor thermal transients of [$]^{a,c,e}$ Nonlinear through wall stress profiles were developed for the remaining severe transients as explained in Section B.1.4. The inside and outside surface stresses calculated by simplified methods for the minor transients are shown in Table B-2. [

$]^{a,c,e}$ This figure shows that the simplified method provides more conservative crack growth.

B.1.4 Nonlinear Stress Distribution for Severe Transients

[

.] a, c, e

B.1.5 OBE Loads

The stresses due to OBE loads were neglected in the fatigue crack growth analysis since these loads are not expected to contribute significantly to crack growth due to small number of cycles.

B.1.6 Total Stress for Fatigue Crack Growth

The total through wall stress at a section was obtained by superimposing the pressure load stresses and the stresses due to deadweight and thermal expansion (normal operating case) on the thermal transient stresses (of Table B-2 or the nonlinear stress distributions discussed in Section B.1.4). Thus, the total stress for fatigue crack growth at any point is given by the following equation:

$$\begin{array}{rclclcl} \text{Total} & & \text{Thermal} & & \text{Stress Due} & & \text{Stress} \\ \text{for} & & \text{Transient} & & \text{to} & & \text{Due to} \\ \text{Fatigue} & = & & + & \text{DW} & + & \text{Internal} & \text{(B.9)} \\ \text{Crack Growth} & & & & \text{Thermal} & & \text{Pressure} \\ & & & & \text{Expansion} & & \end{array}$$

The envelope thermal expansion, deadweight and pressure loads for calculating the total stresses of Equation B.9 are summarized in Table B-3.

B.2 Fatigue Crack Growth Analysis

The fatigue crack growth analysis was performed to determine the effect of the design thermal transients, in Table B-1. The analysis was performed for the critical cross section of the model which is identified in Figure B-2. A range of crack depths was postulated, and each was subjected to the transients in Table B-1.

B.2.1 Analysis Procedure

The fatigue crack growth analyses presented herein were conducted in the same manner as suggested by Section XI, Appendix A of the ASME Boiler and Pressure Vessel Code. The analysis procedure involves assuming an initial flaw exists

at some point and predicting the growth of that flaw due to an imposed series of stress transients. The growth of a crack per loading cycle is dependent on the range of applied stress intensity factor ΔK_I , by the following relation:

$$\frac{da}{dN} = C_0 \Delta K_I^n \quad (B.2.1)$$

where "C₀" and the exponent "n" are material properties, and ΔK_I is defined later, in Equation (B.2.3). For inert environments these material properties are constants, but for some water environments they are dependent on the level of mean stress present during the cycle. This can be accounted for by adjusting the value of "C₀" and "n" by a function of the ratio of minimum to maximum stress for any given transient, as will be discussed later. Fatigue crack growth properties of stainless steel in a pressurized water environment have been used in the analysis.

The input required for a fatigue crack growth analysis is basically the information necessary to calculate the parameter ΔK_I , which depends on crack and structure geometry and the range of applied stresses in the area where the crack exists. Once ΔK_I is calculated, the growth due to that particular cycle can be calculated by Equation (B.2.1). This increment of growth is then added to the original crack size, the ΔK_I adjusted, and the analysis proceeds to the next transient. The procedure is continued in this manner until all the transients have been analyzed.

The crack tip stress intensity factors (K_I) to be used in the crack growth analysis were calculated using an expression which applies for a semi-elliptic surface flaw in a cylindrical geometry [B-4].

The stress intensity factor expression was taken from Reference B-4 and was calculated using the actual stress profiles at the critical section. The maximum and minimum stress profiles corresponding to each transient were input, and each profile was fit by a third order polynomial:

$$\sigma(x) = A_0 + A_1 \frac{x}{t} + A_2 \left(\frac{x}{t}\right)^2 + A_3 \left(\frac{x}{t}\right)^3 \quad (B.2.2)$$

The stress intensity factor $K_I(\phi)$ was calculated at the deepest point of the crack using the following expression:

$$\left[\begin{array}{l} \text{+a,c,e} \\ (2.2.3) \end{array} \right]$$

Calculation of the fatigue crack growth for each cycle was then carried out using the reference fatigue crack growth rate law determined from consideration of the available data for stainless steel in a pressurized water environment. This law allows for the effect of mean stress or R ratio (K_{Imin}/K_{Imax}) on the growth rates.

The reference crack growth law for stainless steel in a pressurized water environment was taken from a collection of data (B-5) since no code curve is available, and it is defined by the following equation:

$$\frac{da}{dN} = [\quad]^{a,c,e} \quad (B.2.4)$$

where $K_{eff} = (K_{Imax}) (1-R)^{1/2}$

$$R = \frac{K_{Imin}}{K_{Imax}}$$

$\frac{da}{dN}$ = crack growth rate in micro-inches/cycle

B.2.2 Results

Fatigue crack growth analyses were carried out for the critical cross section. Analysis was completed for a range of postulated flaw sizes oriented circumferentially, and the results are presented in Table B-4. The postulated flaws are assumed to be six times as long as they are deep. Even for the largest postulated flaw of []^{a,c,e} the result shows that the flaw growth through the wall will not occur during the 40 year design life of the plant. For smaller flaws, the flaw growth is significantly lower. For example, a postulated []^{a,c,e} inch deep flaw will grow to []^{a,c,e} which is less than []^{a,c,e} the wall thickness. These results also confirm operating plant experience. There have been no leaks observed in Westinghouse PWR accumulator lines in over 400 reactor years of operation.

B.3 REFERENCES

- B-1 Westinghouse System Standard Design Criteria 1.3, "Nuclear Steam Supply System Design Transients," Revision 2, April 15, 1974.
- B-2 ASME Section III, Division 1-Appendices, 1983 Edition, July 1, 1983.
- B-3 WECAN -- Westinghouse Electric Computer Analysis, User's Manual -- Volumes 1, II, III and IV, Westinghouse Center, Pittsburgh, PA, Third Edition, 1982.

B-4 McGowan, J. J. and Raymund, M., "Stress Intensity Factor Solutions for Internal Longitudinal Semi-Elliptical Surface Flaws in a Cylinder Under Arbitrary Loadings", Fracture Mechanics ASTM STP 677, 1979, pp. 365-380.

B-5 Bamford, W. H., "Fatigue Crack Growth of Stainless Steel Reactor Coolant Piping in a Pressurized Water Reactor Environment", ASME Trans. Journal of Pressure Vessel Technology, February 1979.

TABLE B-1

THERMAL TRANSIENTS CONSIDERED FOR FATIGUE CRACK GROWTH EVALUATION

Trans. No.	Description	No. of Occurrences	+a,c,e
[]			

TABLE B-2

STRESSES FOR THE MINTOR TRANSIENTS (PSI)

<u>TRANSIENT NO.</u>	<u>NO. OF CYCLES</u>	<u>MAXIMUM INSIDE STRESS</u>	<u>CORRESPONDING OUTSIDE STRESS</u>	<u>MINIMUM INSIDE STRESS</u>	<u>CORRESPONDING OUTSIDE STRESS</u>
					+a,c,e

TABLE B-3

ENVELOPE NORMAL LOADS

CONDITION

Normal Operating



a,c,e

TABLE B-4

ACCUMULATOR LINE FATIGUE CRACK GROWTH RESULTS

Wall Thickness = []

+a,c,e

INITIAL CRACK LENGTH (IN.)	CRACK LENGTH AFTER YEAR			
	10	20	30	40

[]
---	--	--	--	--	---

+a,c,e

+a,c,e



Figure B-1 Comparison of Typical Maximum and Minimum Stress Profile
Computed by Simplified [] +a,c,e

1. [] +a,c,e
2. []

[]

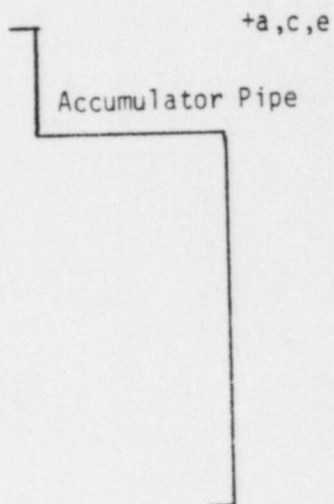


Figure B-2 Schematic of Accumulator Line At
[]

+a,c,e

+a,c,e



+a,c,e

Figure B-3 [] Maximum and Minimum Stress
Profile for Transient #10

+a,c,e

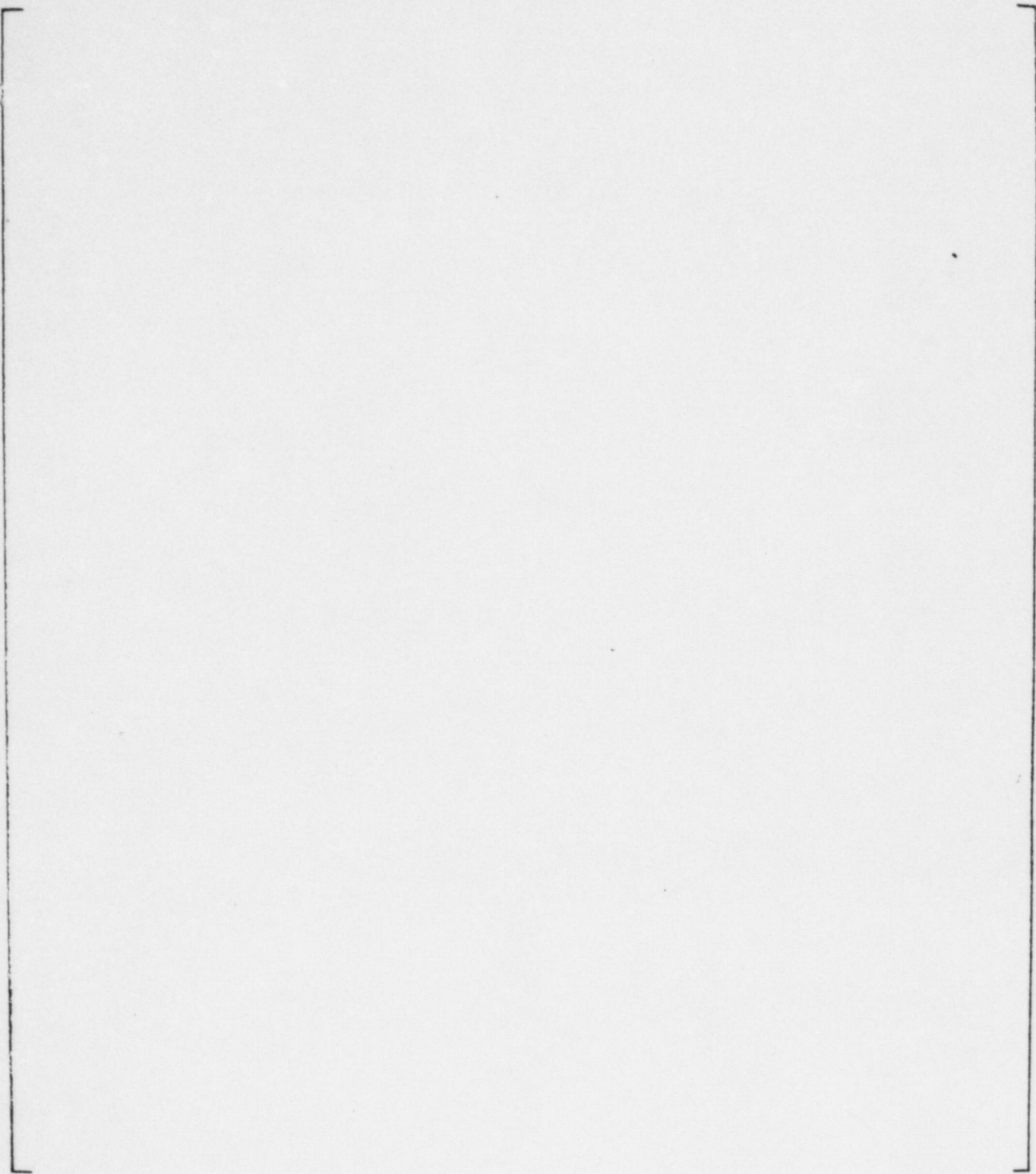


Figure B-4 [

] Maximum and Minimum Stress Profile
for Transient #11

+a,c,e

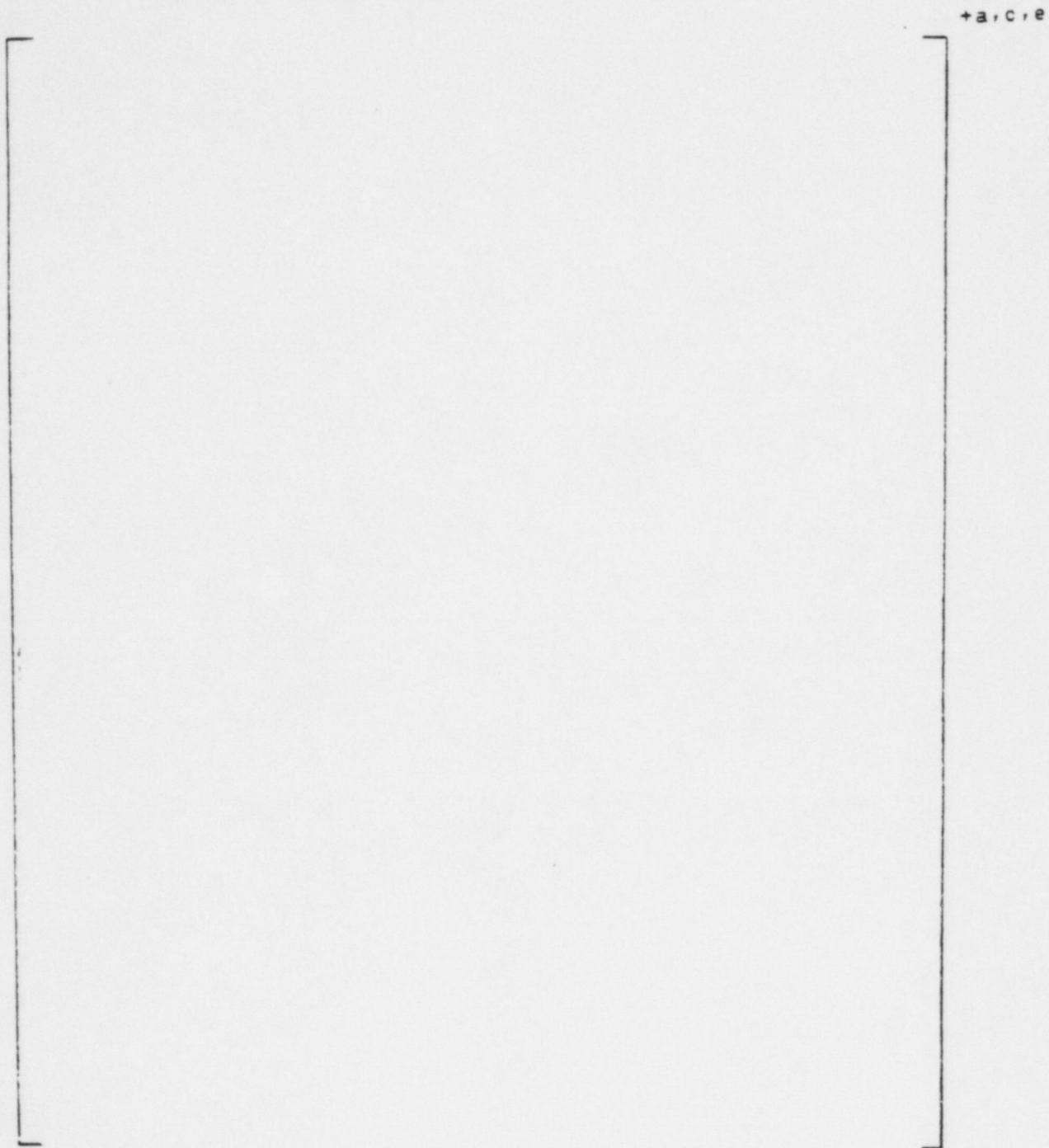


Figure B-5 [] Maximum and Minimum Stress Profile for Transient #12

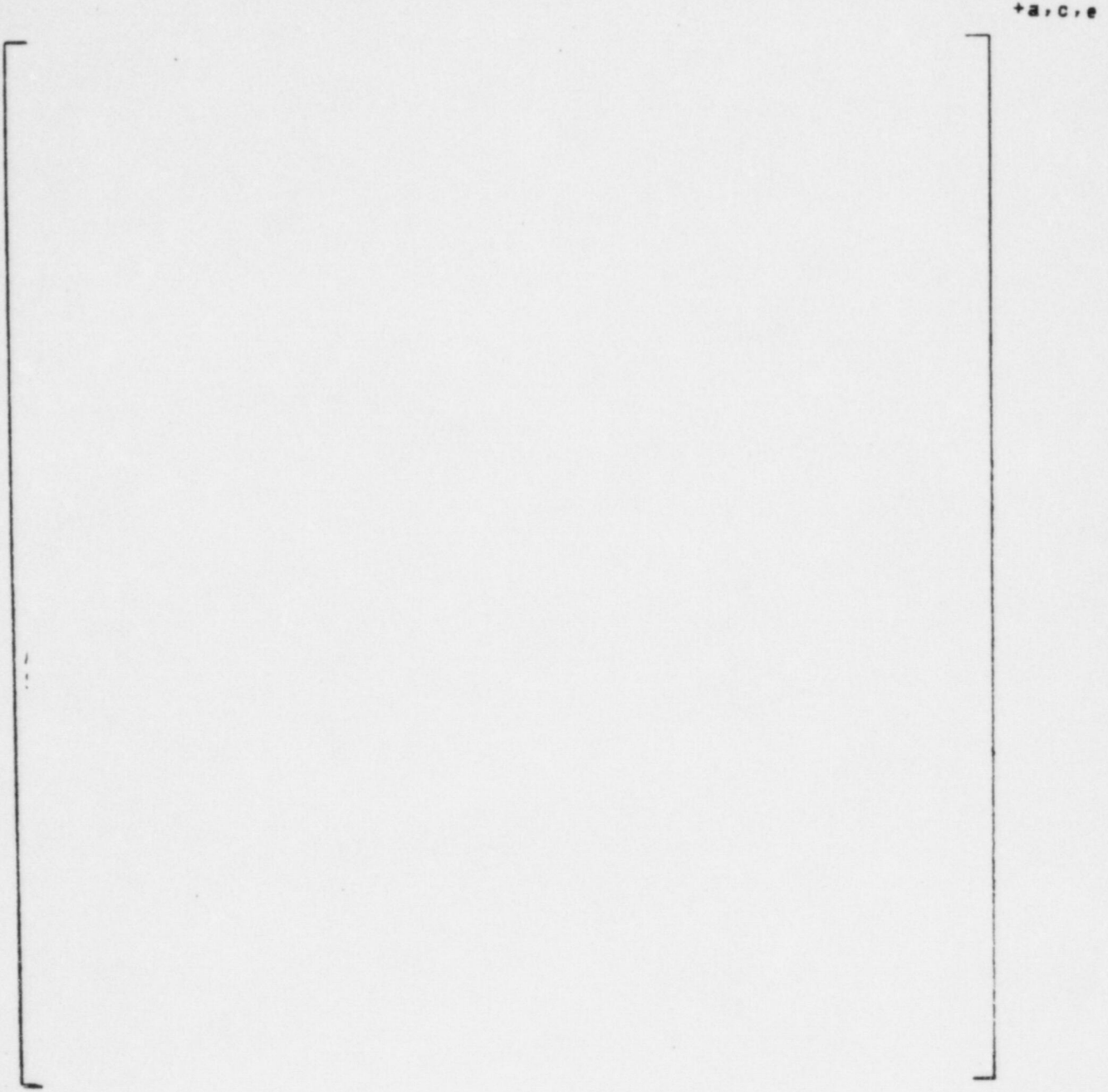


Figure B-6 [] Maximum and Minimum Stress
Profile for Transient #14

+a,c,e